Received: 26 March 2021 | Revised: 9 May 2021 | Accepted: 23 May 2021

DOI: 10.1111/ejn.15325

RESEARCH REPORT

EJN European Journal of Neuroscience FENS WILEY

Different glutamate sources and endogenous co-agonists activate extrasynaptic NMDA receptors on amacrine cells of the rod pathway microcircuit

Pablo Beltrán-Matas | **Espen Hartveit** | **Margaret L. Veruki**

Department of Biomedicine, University of Bergen, Bergen, Norway

Correspondence
Margaret L. Veruki, Department of Biomedicine, University of Bergen, Jonas Lies vei 91, N-5009 Bergen, Norway.
Email: margaret.veruki@uib.no

Funding information
Norges Forskningsråd, Grant/Award Number: 213776 and 261914

Edited by: Ania Majewska

Abstract

The NMDA receptors (NMDARs) expressed by AII and A17 amacrine cells, the two main inhibitory interneurons of the rod pathway microcircuit in the mammalian retina, are exclusively extrasynaptic, activated by ambient levels of glutamate, and molecularly distinct, with AII and A17 amacrines expressing GluN2B- and GluN2A-containing receptors, respectively. This important sensory microcircuit thus provides a unique model to study the activation and function of extrasynaptic NMDARs. Here, we investigated the sources of glutamate and the endogenous co-agonists (D-serine or glycine) that activate these distinct populations of NMDARs. With acute slices from rat retina, we used whole-cell voltage-clamp recording and measurement of current noise to monitor levels of NMDAR activity. Pre-incubation of retina with bafilomycin A1 (an inhibitor of neurotransmitter uptake into synaptic vesicles) abolished NMDAR-mediated noise in AII, but not A17 amacrines, suggesting a vesicular source of glutamate activates AII NMDARs, whereas a non-vesicular source activates A17 NMDARs. Pre-incubation of retina with L-methionine sulfoximine (an inhibitor of glutamine synthetase) also abolished NMDAR-mediated noise in AII, but not A17 amacrines, suggesting a neuronal source of glutamate activates AII NMDARs, whereas a glial source activates A17 NMDARs. Enzymatic breakdown of D-serine reduced NMDAR-mediated noise in AII, but not A17 amacrines, suggesting D-serine is the endogenous co-agonist at AII, but not A17 NMDARs. Our results reveal unique characteristics of these two populations of extrasynaptic NMDARs. The differential and independent activation of these receptors is likely to provide specific contributions to the signal processing and plasticity of the cellular components of the rod pathway microcircuit.

Abbreviations: AMPA, α-amino-3-hydroxy-5-methyl-4-isoxazolepropionic acid; CNQX, 6-cyano-7-nitroquinoxaline-2,3-dione; CPP, (*RS*)-3-(2-carboxypiperazin-4-yl)-propyl-1-phosphonic acid; DAAO, D-amino acid oxidase; DMSO, dimethyl sulfoxide; E_{Cl}, chloride equilibrium potential; GlyT, glycine transporters; INL, inner nuclear layer; I_{NMDA}, NMDAR-mediated current; IPL, inner plexiform layer; IR-DIC, infrared differential interference contrast; MSO, L-methionine sulfoximine; NMDARs, NMDA receptors; ONL, outer nuclear layer; OPL, outer plexiform layer; RBC, rod bipolar cell; R_s, series resistance; spPSCs, spontaneous postsynaptic currents; TBOA, DL-*threo*-b-benzyloxyaspartic acid; TTX, tetrodotoxin.

KEYWORDS
A17 amacrine, AII amacrine, GluN2A, GluN2B, retina

1 | INTRODUCTION

Fast chemical signaling between neurons occurs at morphologically specialized points of contact called synapses, generally containing a high density of neurotransmitter receptors (Cowan & Kandel, 2001). It is clear, however, that neuronal function can be modulated by the activation of so-called extrasynaptic receptors, located away from the synapse (Rusakov & Dityatev, 2014). Extrasynaptic receptors can be involved in volume transmission, where neurotransmitter is released from presynaptic structures with no directly apposed postsynaptic target (Fuxe et al., 2007), or can be activated by neurotransmitter spilling out from the synaptic cleft after release at conventional synapses (Barbour & Häusser, 1997). It has been speculated that the molecular composition of synaptic and extrasynaptic receptors for the same neurotransmitter differ, most likely as an adaptation to differences in magnitude and temporal profile of the neurotransmitter concentration (Muller et al., 2008).

Among ionotropic glutamate receptors, there is evidence that NMDA receptors (NMDARs) can be involved in both synaptic and extrasynaptic neurotransmission (Paoletti et al., 2013; Papouin & Oliet, 2014). It has been suggested that GluN2A subunit-containing receptors primarily have a synaptic location (e.g., Dalby & Mody, 2003) and GluN2B subunit-containing receptors primarily have an extrasynaptic location (e.g., Scimemi et al., 2004). Irrespective of location, the precise subunit composition of NMDARs is of interest because it determines functional properties such as affinity for agonists and co-agonists, single-channel conductance, open probability, kinetics, sensitivity to Mg^{2+}, and magnitude of Ca^{2+} permeability (Monyer et al., 1994; Paoletti et al., 2013). NMDARs are unique in that channel gating requires simultaneous binding of two different ligands, that is, glutamate and a co-agonist (glycine or D-serine), as well as coincident depolarization of the cell membrane to relieve Mg^{2+} block of the channel (Traynelis et al., 2010). In this way, NMDARs function as both ligand- and voltage-gated ion channels, and their high Ca^{2+} permeability allows for an influx of Ca^{2+} that triggers intracellular events, including those related to normal physiological functions such as long-lasting synaptic plasticity, as well as paradoxically, excitotoxicity, and cell death (Paoletti et al., 2013; Papouin & Oliet, 2014). The existence of two different NMDAR co-agonists, glycine, and D-serine, both of which can be present in neural tissue, has lead to the search for the identity and source of the endogenous co-agonist that is involved with specific NMDARs in specific neural circuits (Hansen et al., 2018). Although there are only minor differences between the co-agonists with respect to affinity for NMDARs, the temporal and spatial availability of co-agonist may be a limiting factor for activation of specific NMDARs (Mothet et al., 2015).

In the retina, inhibitory transmission in the rod pathway primarily involves two types of interneurons, AII and A17 amacrine cells, both of which express NMDARs (Hartveit & Veruki, 1997; Veruki et al., 2019; Zhou et al., 2016). AIIs and A17s receive common glutamatergic input from rod bipolar cells at dyad synapses in the proximal inner plexiform layer (Kolb & Famiglietti, 1974; Nelson & Kolb, 1985; Strettoi et al., 1990, 1992). The AII also receives glutamatergic input from OFF-cone bipolar cells at its lobular dendrites in the distal inner plexiform layer (Strettoi et al., 1992). Recent work in our laboratory has suggested that the NMDARs on AII and A17 amacrines are molecularly distinct, containing either GluN2B or GluN2A subunits, respectively, and, for both cell types, these receptors are exclusively extrasynaptic and activated by ambient levels of glutamate (Veruki et al., 2019).

Here, we investigated the sources of glutamate and the identity of the endogenous co-agonists that activate AII and A17 NMDARs. Our results suggest that the glutamate that activates NMDARs on AII amacrines originates from spillover following vesicular (i.e., exocytotic) release from neurons. In contrast, for NMDARs on A17 amacrines, the source of glutamate is non-vesicular, most likely from glial cells. Additionally, our results suggest that D-serine is the primary endogenous co-agonist at NMDARs of AII amacrines, but not at NMDARs of A17 amacrines. That these two extrasynaptic receptor populations are activated by glutamate derived from different sources and released by distinct mechanisms, as well as by different endogenous co-agonists, suggests that each population is able to provide a distinct contribution to excitability and signaling in this microcircuit.

2 | MATERIALS AND METHODS

2.1 | Retinal slice preparation and visual targeting of neurons

General aspects of the methods have previously been described in detail (Veruki et al., 2019). The use of animals in this study was carried out under the approval of and in accordance with the regulations of the Animal Laboratory Facility at the Faculty of Medicine at the University of Bergen (accredited by AAALAC International). Female and male rats (Wistar HanTac; 4–7 weeks postnatal; bred in-house or from

Taconic Bioscience, Denmark) had ad libitum access to food and water and were kept on a 12/12 light/dark cycle. Animals were deeply anaesthetized with isoflurane (IsoFlo vet 100%; Abbott Laboratories) in 100% O_2 and killed by cervical dislocation. After dissection, each retina was cut into four pieces and stored in an interface chamber containing Ames' solution (Sigma-Aldrich) supplemented with 25-mM $NaHCO_3$ to control for pH and bubbled with gas containing 5% CO_2 and 95% O_2. Vertical slices were cut by hand at ~100 to ~150 μm and visualized using an Axioskop 2 FS (Zeiss) with a ×40 water immersion objective and infrared differential interference contrast (IR-DIC) videomicroscopy.

2.2 | Solutions and drugs

The standard extracellular perfusing solution was continuously bubbled with 95% O_2–5% CO_2 and had the following composition (in mM): 125 NaCl, 25 $NaHCO_3$, 2.5 KCl, 2.5 $CaCl_2$, 1 $MgCl_2$, 10 glucose, pH 7.4. To permit observation of NMDAR activity at negative holding potentials, $MgCl_2$ was omitted from the extracellular solution with no replacement of divalent cations (referred to later as Mg^{2+}-free bath solution) to relieve the voltage-dependent block of NMDARs (Nowak et al., 1984). For these recordings, we switched to the Mg^{2+}-free solution at least 10 min before establishing the whole-cell recording configuration for each cell. D-serine, a co-agonist of NMDARs (Kleckner & Dingledine, 1988), was added to the extracellular solution (100 μM; Sigma-Aldrich) as indicated, to either test for saturation of co-agonist binding or ensure adequate levels of co-agonist in the presence of α-amino-3-hydroxy-5-methyl-4-isoxazolepropionic acid (AMPA) receptor blockers that can reduce the release of D-serine in the retina (Stevens et al., 2003; Sullivan & Miller, 2012).

Recording pipettes were filled with (in mM): 125 $CsCH_3SO_3$, 8 NaCl, 10 HEPES, 1 $CaCl_2$, 5 EGTA, 15 TEA-Cl, 4 Mg-ATP (pH adjusted to 7.3 with CsOH). For visualization of complete cellular morphologies with fluorescence microscopy after the recording, Alexa Fluor 594 (40 μM; Invitrogen/Thermo Fisher Scientific) was included in the intracellular solution. Drugs were added directly to the extracellular solution at the following concentrations (supplied by Hello Bio, unless otherwise indicated): 1-μM strychnine (Research Biochemicals International); 10-μM (−)-bicuculline methochloride (Tocris Bioscience); 0.3- or 1-μM tetrodotoxin (TTX); 10-μM 6-cyano-7-nitroquinoxaline-2,3-dione (CNQX); 20-μM (*RS*)-3-(2-carboxypiperazin-4-yl)-propyl-1-phosphonic acid (CPP); 50-μM 0.05 DL-*threo*-β-benzyloxyaspartic acid TBOA; 0.29 U/ml D-amino acid oxidase (DAAO; Merck). DAAO was perfused for at least 20 min before measurements were made (cf. Kalbaugh et al., 2009).

For some experiments, prior to cutting slices and electrophysiological recording, pieces of retina were incubated by submersion for 2.5–4 hr in a small volume (~1 ml) of Ames' solution (with 25-mM $NaHCO_3$ to control for pH and bubbled with 5% CO_2 and 95% O_2) and either 4-μM bafilomycin A1 (henceforth referred to as bafilomycin; Hello Bio) or 5-mM L-methionine sulfoximine (MSO; Sigma-Aldrich). Bafilomycin was first dissolved in dimethyl sulfoxide (DMSO; Sigma-Aldrich) at a concentration of 1 mM before dilution to the final concentration in Ames' solution. As a control, we incubated retina tissue in Ames' solution (as above) with 0.4% DMSO (equal to the final concentration of DMSO in the solution with bafilomycin).

2.3 | Electrophysiological recording, data acquisition, and imaging

Patch pipettes were pulled from thick-walled borosilicate glass (BF150-86–10; Sutter Instrument) to obtain an open-tip resistance that ranged from 5 to 8 MΩ when filled with intracellular solution. Whole-cell voltage-clamp recordings were performed with an EPC9-dual amplifier controlled with Patchmaster software (HEKA Elektronik). The data acquisition software corrected all holding potentials (V_h) for liquid junction potentials on-line. Theoretical liquid junction potentials were calculated with JPCalcW (Axon Instruments). In all experiments, AII and A17 amacrine cells were held at a membrane potential of −60 or −70 mV, respectively. For whole-cell recordings, series resistance (R_s) was monitored throughout the recording (for details, see Castilho et al., 2015). Cells with $R_s > 45$ MΩ were not included in the final material.

To examine NMDAR activity and the influence of different pharmacological manipulations, we measured membrane current noise, that is, the variance of the current recorded in the whole-cell voltage-clamp configuration (Sah et al., 1989; Veruki et al., 2019). Current variance was calculated for 20-s epochs of continuous recording interrupted by intervals of ~15 s where we sampled responses for calculating R_s. The variance from two to four such epochs was averaged for any given condition. The sampling interval was set to 500 μs, and the corner frequency (−3 dB) of the low-pass filter was set to 952.4 Hz (Butterworth), corresponding to a ratio of 2.1 between the sampling and corner frequencies (for details, see Veruki et al., 2019).

In some cases, image stacks of amacrine cells filled with fluorescent dye were acquired using a digital CCD camera (CoolSnap ES; Photometrics/Roper Scientific) controlled by μManager software (www.micro-manager.org) running under Windows XP. During image acquisition, exposure to UV light was controlled by an electronic shutter (Uniblitz VCM-D1, Vincent Associates) to minimize the total exposure time.

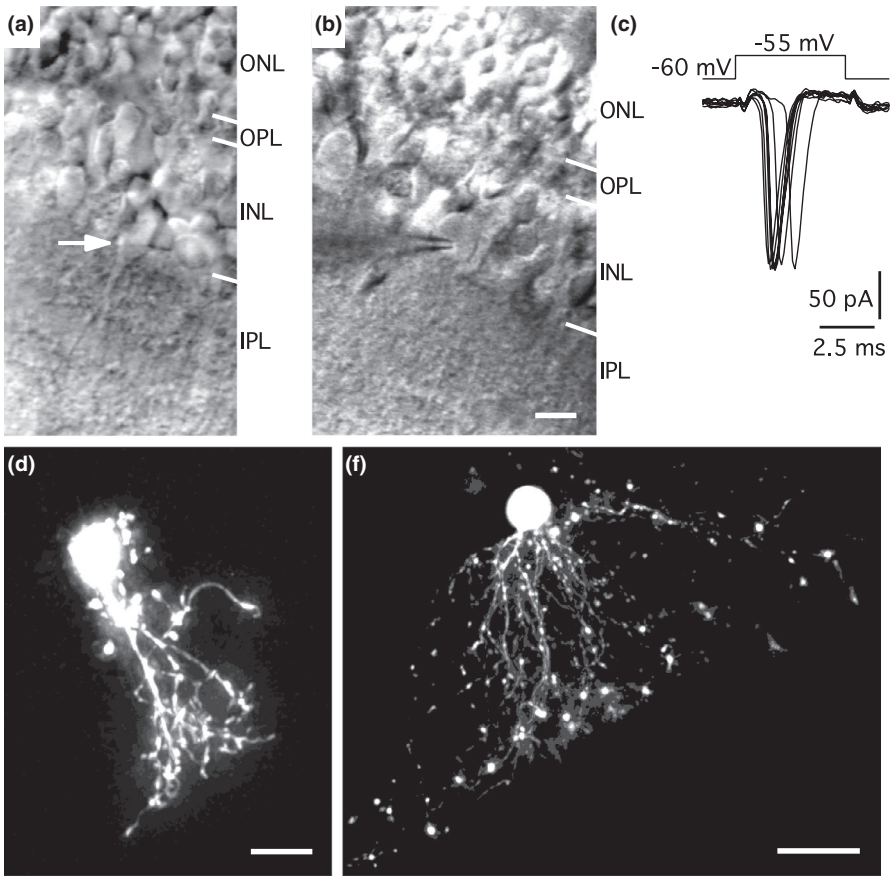

FIGURE 1 Identification of AII and A17 amacrine cells in the rat retinal slice. (a) IR-DIC videomicrograph of a retinal slice with cell body (arrow) and apical dendrite of an AII amacrine. Here and in (b), the retinal layers are indicated by abbreviations and the borders between layers are marked by lines aligned with their orientation (ONL, outer nuclear layer; OPL, outer plexiform layer; INL, inner nuclear layer; IPL, inner plexiform layer). (b) IR-DIC videomicrograph of a retinal slice with cell body of an A17 amacrine (with pipette attached). Scale bar: (a, b) 10 µm. (c) Electrophysiological "signature" of AII amacrine cell during whole-cell voltage-clamp recording. Transient inward currents (bottom traces) correspond to unclamped action currents (escape from voltage clamp) evoked by 5 mV depolarizing voltage pulses from $V_h = -60$ mV (top trace). (d) Wide-field fluorescence image of AII amacrine filled with Alexa 594 via patch pipette, maximum intensity projection of image stack after deconvolution. Scale bar: 10 µm. (e) Wide-field fluorescence image of A17 amacrine filled with Alexa 594 via patch pipette, maximum intensity projection of image stack after deconvolution. Scale bar: 20 µm

Deconvolution of image stacks and generation of maximum intensity projections were performed as described in Zandt et al. (2017). Final adjustments of contrast and brightness were applied homogeneously over the entire image.

2.4 | Experimental design and statistical analysis

Electrophysiological data were analyzed with Fitmaster (HEKA Elektronik), IGOR Pro (WaveMetrics), and Excel (Microsoft). Data are presented as mean ± *SEM* (n = number of cells) with ranges either displayed by individual data points in bar graphs or stated explicitly. We did not perform prior sample size calculations for these experiments, which are relatively time-consuming and difficult to perform. Instead, each cell served as its own control and we used all the cells from which we obtained high-quality recordings, within a reasonable time frame, making sure that each cell type was covered by at least three cells for each experiment. Statistical analyses were performed in Prism 6 (GraphPad Software) using ratio paired t tests (two-tailed) or ANOVA (one-way or two-way), as indicated. The ratio paired t test is appropriate when there is reason to believe that the relative difference is a more consistent measure than the absolute difference. Differences were considered statistically significant at the $p < 0.05$ level. Exact p values are given in the text or in the figure legends. Unless otherwise noted, the current traces shown in the figures represent individual traces. Altogether, recordings from 25 AII and 32 A17 amacrine cells are presented, including four A17 amacrine cells tested with TBOA (originally published in Veruki et al., 2019) that were re-analyzed and compared with the A17 amacrines tested with TBOA after incubation in MSO.

3 | RESULTS

3.1 | Identification of AII and A17 amacrine cells in retinal slices

Both AII and A17 amacrine cells can be visually targeted in the retinal slice. The primary targeting criterion was the shape and location of the cell bodies at the border between the inner nuclear layer and the inner plexiform layer (Figure 1a,b). The AII amacrine has an elongated cell body that spans the border between the inner nuclear layer and the inner plexiform layer and a thick apical dendrite that tapers as it descends into the inner plexiform layer (Figure 1a). In contrast, the A17 amacrine has a dome-shaped cell body, with the flat surface located at the border between the inner nuclear layer and the inner plexiform layer (Figure 1b). Following establishment of the whole-cell configuration for AII amacrines, we verified that 5-mV depolarizing pulses (from $V_h = -60$ mV, 5 ms) evoked characteristic inward action currents mediated by TTX-sensitive voltage-gated Na^+ channels (Figure 1c; Mørkve et al., 2002). For unequivocal identification, all recorded cells were visualized with fluorescence microscopy following the recording. The AII is a bi-stratified, narrow-field amacrine cell (Figure 1d), and the A17 is a diffuse, wide-field amacrine cell with long, thin processes that carry distinct varicosities and terminate near the ganglion cell layer of the retina (Figure 1e).

3.2 | Depletion of neurotransmitter from synaptic vesicles reduces activation of NMDARs on AII, but not A17 amacrines

We have previously demonstrated that ambient glutamate can activate NMDARs on both AII and A17 amacrine cells (Veruki et al., 2019). However, the source of this extracellular glutamate is not known and could be either neuronal or glial, or both. To differentiate between neuronal and glial sources of glutamate, we first examined the effect of bafilomycin, an inhibitor of the vacuolar ATPase that establishes the proton gradient that drives neurotransmitter uptake into synaptic vesicles (Dröse & Altendorf, 1997). For these experiments, we incubated pieces of retina in bafilomycin (4 μM) for at least 2.5 hr before preparing vertical slices for electrophysiological recording. Because bafilomycin prevents uptake of neurotransmitter into synaptic vesicles, the continuous baseline exocytosis of vesicles will effectively deplete the vesicles of neurotransmitter (Cavelier & Attwell, 2007; Harrison & Jahr, 2003; Le Meur at al., 2007; Wu et al., 2012; Zhou et al., 2000).

A relatively long-lasting incubation of the retina by submersion (with bafilomycin or MSO, see below) prior to recording introduced a new element in our experimental paradigm compared with similar experiments from our laboratory (cf. Veruki et al., 2019). We therefore first verified that NMDARs on AII and A17 amacrines could still be activated by ambient glutamate after a similar incubation of tissue in control Ames' solution for the same period of time (at least 2.5 hr). For these experiments, CNQX, strychnine, bicuculline, and TTX (to block AMPA, glycine, and $GABA_A$ receptors and voltage-gated Na^+ channels, respectively) were included in the bath solution during electrophysiological recording. For the AII amacrine illustrated in Figure 2a, applying the NMDAR antagonist CPP markedly decreased the membrane current noise (measured as variance), from an average of 89.3 pA^2 in control to 4.4 pA^2 in CPP (a reduction of 95%). For a total of four AII amacrines, the average membrane current noise in control was 50.4 ± 20.6 pA^2. This was reduced to 6.4 ± 2.2 pA^2 in CPP (average reduction of $79 \pm 7\%$; $p = 0.0291$, ratio paired t test; $n = 4$; Figure 2b). Similar experiments were performed with A17 amacrines. For the A17 illustrated in Figure 2c, applying CPP markedly decreased the current noise, from an average of 5.7 pA^2 in control to 0.5 pA^2 in CPP (a reduction of 92%). For a total of three A17 amacrines, the average current noise in control was 3.1 ± 1.3 pA^2. This was reduced to 0.4361 ± 0.0045 pA^2 in CPP (average reduction of $80 \pm 7\%$; $p = 0.0457$, ratio paired t test; $n = 3$; Figure 2d). These results corresponded well to our previous findings (Veruki et al., 2019) and confirmed that gating of NMDAR channels contributed substantially to current noise in the baseline condition of the present study.

We next recorded from AII and A17 amacrines in retinal slices prepared from tissue that had been incubated in bafilomycin. These recordings were performed without blockers of neurotransmitter receptors. As illustrated by the examples in Figure 3a,b, incubation in bafilomycin almost completely eliminated synaptic currents and strongly reduced current noise (AII: Figure 3a, *upper trace*; A17: Figure 3b, *upper trace*), as expected from disrupted loading of synaptic vesicles by bafilomycin. This contrasted strongly with recordings from AII and A17 amacrines (also performed without blockers of neurotransmitter receptors) from tissue incubated under identical conditions, but without the addition of bafilomycin (Figure 3a,b, *lower traces*). With the intracellular and extracellular solutions used here, the chloride equilibrium potential (E_{Cl}) was ~−60 mV. Accordingly, with V_h at either −60 mV (AIIs) or −70 mV (A17s), there was essentially no driving force for chloride current through GABA and/or glycine receptor channels and the synaptic activity most likely corresponded to spontaneous excitatory postsynaptic currents mediated by AMPA-type glutamate receptors (Veruki et al., 2003). These results suggested that after incubation in bafilomycin, exocytosis of synaptic vesicles was not accompanied by release of neurotransmitter.

If the source of ambient glutamate that activates the extrasynaptic NMDARs is generated by release from synaptic

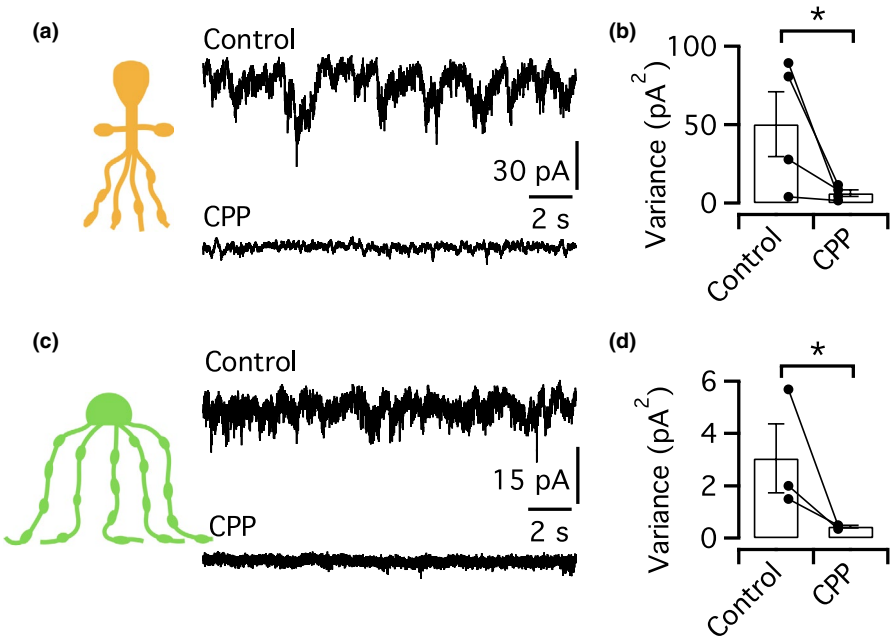

FIGURE 2 Activation of NMDARs by ambient glutamate generates membrane current noise in AII and A17 amacrines. (a) Current of an AII amacrine recorded in whole-cell voltage clamp ($V_h = -60$ mV) in control (upper trace) and during application of CPP (20 μM) in the bath solution (lower trace) to block NMDARs. Here and later (unless otherwise noted), "control" refers to Mg^{2+}-free bath solution that includes D-serine (100 μM) and blockers of AMPA, $GABA_A$, and glycine receptors and voltage-gated Na^+ channels (see Section 2). Note reduction of current noise by CPP, suggesting activation of NMDARs by ambient glutamate in the control condition. Here and later, the identity of the cell (AII or A17) from which the recording was performed is indicated by the schematic figure next to the current traces. (b) Bar graph displays membrane current noise measured as variance (here and later, bars represent mean ± *SEM*) in AII amacrines ($n = 4$ cells) in control (without CPP; left bar) and in CPP (right bar). Here and later, data points for the same cell are connected by lines and the results from statistical comparisons between averages are indicated by n.s. (no significant difference, $p > 0.05$) or a single asterisk (*; statistically significant difference, $p \leq 0.05$). (c) Current from an A17 amacrine recorded in whole-cell voltage clamp ($V_h = -70$ mV) in control (upper trace) and during application of CPP (20 μM) in the bath solution (lower trace). Note reduction of current noise by CPP, suggesting activation of NMDARs by ambient glutamate in the control condition. (d) Bar graph displays membrane current noise measured as variance in A17 amacrines ($n = 3$ cells) in control and in CPP

vesicles, we would expect that blocking these receptors pharmacologically should have little effect on membrane current noise in cells recorded from tissue incubated in bafilomycin. To test this, we measured current noise in AII amacrines after incubation in bafilomycin both before (control) and after adding CPP. For these experiments, CNQX, strychnine, bicuculline, and TTX were included in the bath solution. For the AII amacrine illustrated in Figure 3c, adding CPP had almost no effect on the current noise, with an average of 2.8 pA^2 in control and 2.6 pA^2 in CPP (a reduction of only 7%). For a total of five AII amacrines, the average current noise in control was 3.20 ± 0.97 pA^2, not significantly different from 2.45 ± 0.72 pA^2 in CPP (an average reduction of 16%; $p = 0.3209$, ratio paired *t* test; $n = 5$; Figure 3d). This result was, however, significantly different compared with the strong reduction of current noise evoked by CPP in AIIs from tissue that had not been incubated in bafilomycin (where the average reduction was 79%), as can be seen by comparing Figure 2b with Figure 3d ($F_{1,7} = 6.246$, $p = 0.0410$, two-way ANOVA). These results suggested that incubation in bafilomycin, by blocking vesicular release of neurotransmitter, strongly reduced the level of extracellular glutamate available to activate the extrasynaptic NMDARs on AII amacrines.

In contrast, for A17 amacrines recorded from tissue that had been incubated in bafilomycin, the membrane current noise was still markedly reduced after adding CPP. For the A17 amacrine illustrated in Figure 3e, the noise was reduced from 1.5 pA^2 in control to 0.4 pA^2 in CPP (a reduction of 72%). For a total of five A17 amacrine cells, the average current noise in control was 1.05 ± 0.20 pA^2, and in CPP, it was significantly reduced to 0.53 ± 0.12 pA^2 (an average reduction of 46%; $p = 0.0182$, ratio paired *t* test; $n = 5$; Figure 3f). Furthermore, this reduction of current noise was not significantly different from that evoked by CPP in A17s from tissue that had not been incubated in bafilomycin (where the average reduction was 80%), as can be seen by comparing Figure 2d with Figure 3f ($F_{1,6} = 4.528$, $p = 0.0761$, two-way ANOVA). Thus, incubation in bafilomycin did not significantly disrupt the source of glutamate that activates extrasynaptic NMDARs on A17 amacrines. This suggested that the source of glutamate for these receptors is predominantly non-vesicular.

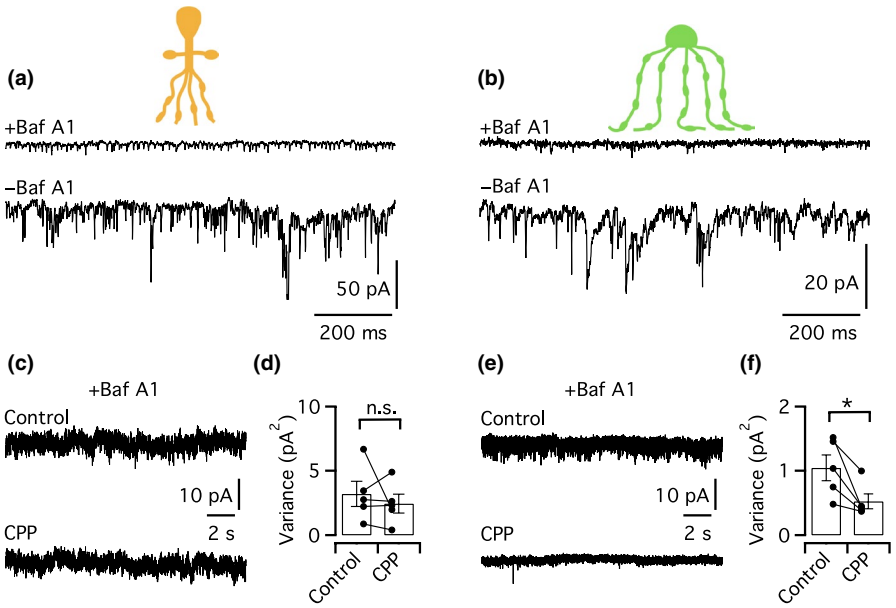

FIGURE 3 Depletion of neurotransmitter from synaptic vesicles with bafilomycin A1 reduces NMDAR activation in AII, but not A17 amacrines. (a) Upper trace: current from an AII amacrine from tissue incubated with bafilomycin A1 (Baf A1; 4 μM) for >2.5 hr prior to slice preparation. Note lack of spontaneous postsynaptic currents (spPSCs) and low membrane current noise. Lower trace: current from a different AII amacrine recorded under identical conditions, but from tissue incubated without Baf A1. Note spPSCs and prominent current noise. (b) Upper trace: current from an A17 amacrine from tissue incubated with Baf A1 for >2.5 hr prior to slice preparation. Note lack of spPSCs and low current noise. Lower trace: current from a different A17 amacrine recorded under identical conditions, but from tissue incubated without Baf A1. Note spPSCs and prominent current noise. (c) Current from an AII amacrine from tissue incubated with Baf A1, both in control (without CPP; upper trace) and after adding CPP (20 μM) to the bath solution (lower trace). Note similar magnitude of current noise in the two conditions. (d) Bar graph displays membrane current noise measured as variance in AII amacrines ($n = 5$ cells) in control and in CPP. Note lack of effect of CPP on current noise. (e, f) same as (c, d), but for A17 amacrines ($n = 5$ cells). Note significant reduction of current noise by CPP in A17s from tissue incubated in Baf A1

3.3 | Disruption of the glutamate-glutamine cycle reduces NMDAR activation in AII, but not A17 amacrines

Under normal conditions in the nervous system, a glutamate-glutamine cycle operates where glial cells take up glutamate from the extracellular environment, convert it to glutamine with the enzyme glutamine synthetase, and then release the glutamine, which is subsequently taken up by neurons and converted back to glutamate (reviewed in Schousboe, 2019). In the retina, glutamine synthetase is located exclusively in Müller glial cells (Lewis et al., 1988; Riepe & Norenburg, 1977), and treatment with MSO leads to a rapid and complete redistribution of glutamate from neurons to Müller cells (Barnett et al., 2000; Pow & Robinson, 1994; Winkler et al., 1999). In hippocampal slices, inhibiting glutamine synthetase with MSO has also been shown to redistribute glutamate, resulting in a decrease of glutamate in neuronal terminals and an increase of glutamate in glial cells (Laake et al., 1995). Thus, MSO will both eliminate the ability of neurons to replenish the glutamate used for synaptic release and potentially increase the glutamate available for release from glial cells due to intracellular accumulation. We reasoned that if the extracellular glutamate that activates extrasynaptic NMDARs on AII and A17 amacrines was from a neuronal source, inhibiting glutamine synthetase with MSO would have an effect similar to bafilomycin (by decreasing the glutamate available to activate the receptors). However, if the NMDARs are activated by glutamate released from glial cells, inhibiting glutamine synthetase with MSO should not reduce the available glutamate and, thus, should not lead to a reduced activation of the receptors.

To test these predictions, we inhibited glutamine synthetase by incubating pieces of retina in MSO for at least 2.5 hr (Le Meur et al., 2007; Wu et al., 2012) before preparing retinal slices and recording from AII and A17 amacrines. As illustrated by the examples in Figure 4a,b, incubation in MSO almost completely eliminated synaptic currents and strongly reduced current noise in both cell types, in recordings without blockers of neurotransmitter receptors (Figure 4a,b, *upper traces*). This contrasted strongly with similar recordings from AII and A17 amacrines incubated under identical conditions, but without the addition of MSO (Figure 4a,b, *lower traces*). This result was consistent with a disruption of the glutamate-glutamine cycle by MSO.

We next investigated the effect of blocking NMDARs in cells recorded from tissue incubated in MSO, by measuring membrane current noise before (control) and after adding

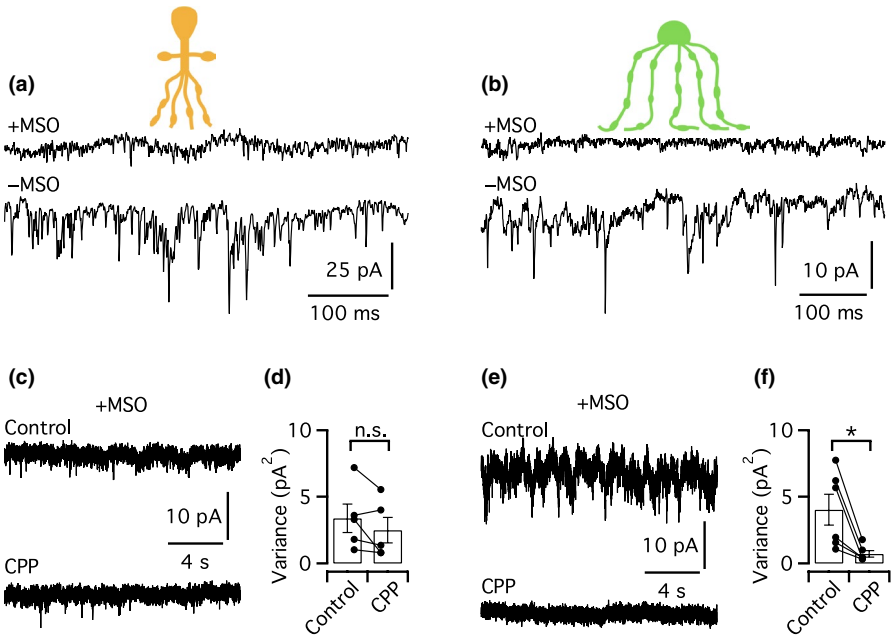

FIGURE 4 Blocking glutamine synthetase with MSO reduces NMDAR activation in AII, but not A17 amacrines. (a) Upper trace: current from an AII amacrine from tissue incubated with MSO (5 mM) for >2.5 hr prior to slice preparation. Note lack of spPSCs and low current noise. Lower trace: current from a different AII amacrine recorded under identical condtions, but from tissue incubated without MSO. Note spPSCs and prominent current noise. (b) Upper trace: current from an A17 amacrine from tissue incubated with MSO for >2.5 hr prior to slice preparation. Note complete lack of spPSCs and low current noise. Lower trace: current from an A17 amacrine recorded under identical conditions, but from retinal tissue incubated without MSO. Note spPSCs and prominent current noise. (c) Current from an AII amacrine from tissue incubated with MSO, both in control (without CPP; upper trace) and after adding CPP (20 μM) to the bath solution (lower trace). Note similar magnitude of current noise in the two conditions. (d) Bar graph displays membrane current noise measured as variance in AII amacrines ($n = 5$ cells) in control and in CPP. Note lack of effect of CPP on current noise. (e, f) same as (c, d), but for A17 amacrines ($n = 6$ cells). Note significant reduction of current noise by CPP in A17 amacrines from tissue incubated in MSO

CPP. For these experiments, CNQX, strychnine, bicuculline, and TTX were included in the bath solution. For the AII amacrine illustrated in Figure 4c, from tissue incubated in MSO, adding CPP had almost no effect on the current noise, with an average of 1.0 pA^2 in control and 0.8 pA^2 in CPP. For a total of five AII amacrines, the average current noise in CPP was 2.53 ± 0.95 pA^2, slightly reduced, but not significantly different from 3.3 ± 1.1 pA^2 in control ($p = 0.11418$, ratio paired t test; $n = 5$; Figure 4d). However, the average reduction of current noise (24%) evoked by CPP in AIIs from tissue incubated in MSO was significantly different from that evoked by CPP in AIIs from tissue not incubated in MSO (a 79% reduction in noise), as can be seen by comparing Figure 2b with Figure 4d ($F_{1,7} = 6.274$, $p = 0.0407$, two-way ANOVA). Thus, MSO disrupted the source of glutamate that activates extrasynaptic NMDARs of AII amacrines, suggesting that the source of glutamate is neuronal and not glial in origin.

In contrast, for A17 amacrines recorded from tissue incubated in MSO, adding CPP markedly reduced the membrane current noise. For the A17 amacrine illustrated in Figure 4e, the noise was reduced from 6.2 pA^2 in control to 1.0 pA^2 in CPP (a reduction of 84%). For a total of six A17 amacrine cells, the average current noise in control was 4.0 ± 1.2 pA^2, and in CPP, it was significantly reduced to 0.72 ± 0.24 pA^2 (an average reduction of 79%; $p = 0.0008$, ratio paired t test; $n = 6$; Figure 4f). This strong reduction of current noise was not significantly different from that evoked by CPP in A17s from tissue not incubated in MSO (where the average reduction was 80%), as can be seen by comparing Figure 2d with Figure 4f ($F_{1,7} = 0.1740$, $p = 0.6891$, two-way ANOVA). Thus, depleting neuronal glutamate by blocking glutamine synthetase with MSO had no effect on the activity of the extrasynaptic NMDARs on A17 amacrines. This strongly suggested that the source of glutamate for these receptors is glial in origin.

Next, we considered that an MSO-evoked redistribution of glutamate from neurons to Müller glial cells (Barnett et al., 2000; Pow & Robinson, 1994; Winkler et al., 1999), could increase the glutamate accumulated in and released from the glial cells, and thus lead to an enhanced activation of NMDARs on A17 amacrines. An increased activation of NMDARs, however, could be prevented if glutamate transporters are able to effectively buffer increased extracellular glutamate (Le Meur et al., 2007). To investigate this, we repeated the above experiments and recorded from A17 amacrines in tissue that had been incubated in MSO. For these recordings, CNQX, strychnine, bicuculline, and TTX were included in the bath solution. After establishing a baseline

of current noise, we blocked uptake of glutamate by adding TBOA, a non-selective, non-transported blocker of excitatory amino acid transporters (Shimamoto et al., 1998), to the bath solution. For the A17 illustrated in Figure 5a, TBOA evoked a large inward current (~70 pA) and a strong increase of current noise, from 9.1 pA^2 in control to 38.4 pA^2 in TBOA (an increase of ~320%; Figure 5a,b). Adding CPP (in the maintained presence of TBOA) blocked the increase of current noise, reducing it to a level (1.1 pA^2) that was much lower than the baseline level observed before adding TBOA (Figure 5a,b). CPP also blocked the inward current evoked by TBOA, resulting in an apparent outward current relative to the baseline recorded before TBOA (Figure 5a). This suggested that NMDARs were activated in the baseline condition and that the level of activation increased after blocking glutamate uptake pharmacologically.

The difference between the maximum inward current during TBOA (relative to baseline) and the maximum outward current during CPP (relative to baseline) corresponds to the total NMDAR-mediated current (I_{NMDA}; Figure 5a). For this cell, I_{NMDA} measured ~105 pA. Similar results were observed for a total of six A17s incubated in MSO. Adding

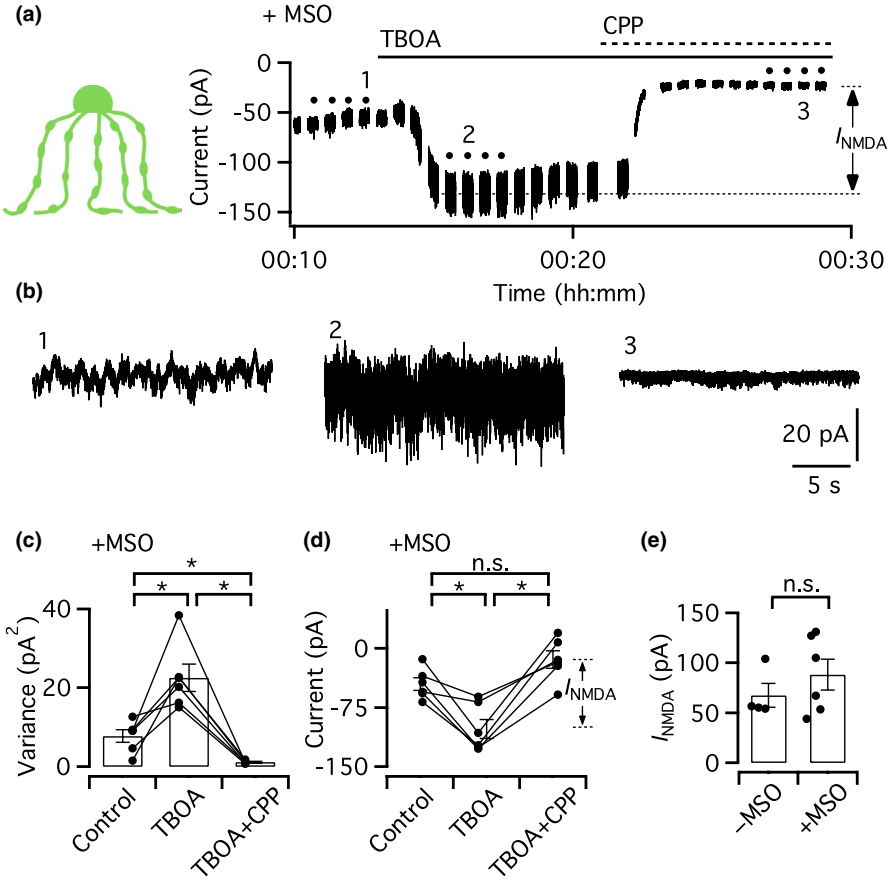

FIGURE 5 Incubation in MSO does not result in increased glutamate release from glial cells. (a) Series of 20-s epochs of current recorded from an A17 amacrine from tissue incubated with MSO (5 mM; >2.5 hr) before slice preparation. After establishing a baseline, TBOA (50 μM) was added to the bath solution (here and later, duration of drug application indicated by continuous or dashed horizontal line above current traces) to block uptake of glutamate. Note inward current (relative to baseline) and increased noise evoked by TBOA. Subsequently, CPP (20 μM) was added to the bath solution to block NMDARs. Note block of inward current and strong reduction of current noise by CPP. Here and later, black circles above recorded currents indicate epochs used to calculate averages for current amplitude and current noise for a given condition. Here and later, numbered data points (1, 2, and 3) correspond to current epochs displayed separately with expanded time axis. Here and in (d) vertical line marked I_{NMDA} is the difference between the maximum inward current (relative to basline) in TBOA and maximum outward current (relative to baseline) in CPP and corresponds to current activated by endogenous agonist (presumably glutamate) mediated by NMDA receptor channels. (b) Individual epochs of current recorded from A17 amacrine in (a); in control (1), in the presence of TBOA (2), and in the presence of TBOA + CPP (3). (c) Bar graph displays membrane current noise measured as variance in A17 amacrines ($n = 6$ cells) recorded from tissue incubated with MSO before slice preparation in control, in TBOA, and in TBOA + CPP. Note significant differences between noise in the three conditions. (d) Current amplitude in A17 amacrines (same cells as in c) measured in the same conditions as in (c): control, TBOA, and TBOA + CPP. Note inward current evoked by TBOA and subsequent block by CPP. (e) Bar graph displays I_{NMDA} (estimated as indicated in a and d) in A17 amacrine cells from tissue incubated without (−MSO) or with (+MSO) MSO. Note no significant difference in I_{NMDA} between the two conditions

TBOA significantly increased the average current noise from 7.7 ± 1.6 pA^2 in the baseline condition to 22.5 ± 3.4 pA^2 (an increase of ~370%; Figure 5c; $p = 0.0235$, adjusted p value, one-way ANOVA followed by Tukey's multiple comparison test; $n = 6$). Adding CPP reduced the average noise to 1.15 ± 0.16 pA^2, a significant decrease from both the baseline condition (75% reduction, $p = 0.0221$) and the TBOA condition (95% reduction, $p = 0.0035$; adjusted p values, one-way ANOVA followed by Tukey's multiple comparison test; $n = 6$). For the same cells, TBOA evoked a net inward current of 57 ± 13 pA (range 13−94 pA) relative to control, from −45.4 ± 7.8 pA in control to −102 ± 12 pA in TBOA ($p = 0.0166$, adjusted p value, one-way ANOVA followed by Tukey's multiple comparison test; $n = 6$; Figure 5d). Adding CPP blocked the inward current evoked by TBOA and for the majority of cells also evoked an apparent outward current relative to baseline (Figure 5d). The average current after adding CPP was −14 ± 11 pA, significantly different from the TBOA condition ($p = 0.0055$), but not significantly different from the control condition ($p = 0.1092$, adjusted p values, one-way ANOVA followed by Tukey's multiple comparison test; $n = 6$; Figure 5d). The average I_{NMDA} for A17 amacrines from tissue incubated in MSO was 88 ± 16 pA ($n = 6$), not significantly different from I_{NMDA} for A17s that had not been exposed to MSO (67 ± 12 pA; $n = 4$; $p = 0.3673$, unpaired t test; Figure 5e). This suggested that if incubation in MSO increases the glutamate available for release from glial cells, it does not result in increased activation of NMDARs on A17 amacrine cells. These results also suggested that incubation in MSO does not in itself block the activity of glutamate transporters and, that for A17 amacrines, I_{NMDA} is independent of synaptically released glutamate. Taken together, these experiments provide additional strong support for the hypothesis that NMDARs on A17s are activated by glutamate released from a glial source.

3.4 | Co-agonist binding sites are not saturated for NMDARs of AII or A17 amacrines

Unlike most neurotransmitter receptors, NMDARs require the binding of a co-agonist, either glycine or D-serine, for channel gating to occur (Johnson & Ascher, 1987; Kleckner & Dingledine, 1988; Mothet et al., 2000; Wolosker et al., 1999). To explore the role of the co-agonist binding site for the NMDARs of AII and A17 amacrines, we first addressed whether the endogenous co-agonist binding sites are saturated in our preparation. To investigate this we recorded membrane current noise, first in a control condition without D-serine in the bath solution and then after adding D-serine (100 μM) to the bath solution. In these experiments, CNQX, bicuculline, strychnine, and TTX were included in the bath solution. For the AII amacrine illustrated in Figure 6a, the current noise increased from 15.0 pA^2 in control to 25.9 pA^2 in D-serine (an increase of ~72%; each average calculated from four epochs, Figure 6a). The increase of noise can be seen more clearly for the representative epochs illustrated at an expanded scale in Figure 6b (1: control, 2: D-serine). For this cell, D-serine also evoked a small inward current relative to baseline (~3 pA). For a total of six AIIs tested, there was a significant increase of current noise from 21.2 ± 6.7 pA^2 in control to 35 ± 11 pA^2 in the presence of D-serine (an average increase of ~68%; $p = 0.0163$, ratio paired t test, $n = 6$; Figure 6c). D-serine did not, however, evoke a significant or consistent change in current amplitude, with a small inward current observed for three cells and a small outward current for the three other cells (the average net change was 4.6 ± 7.2 pA).

When A17 amacrines were tested in the same way, the results were similar to but much more pronounced than for the AIIs. For the A17 illustrated in Figure 6d, the current noise increased from 2.6 pA^2 in control to 26.7 pA^2 in D-serine (an increase of ~925%; each average calculated from two or three epochs as indicated; Figure 6d). The strong increase of noise can be seen more clearly for the representative epochs illustrated at an expanded scale in Figure 6e (1: control, 2: D-serine). The increase of noise was accompanied by a large inward current with both transient and sustained components (~42 pA peak amplitude relative to the baseline level). Adding CPP (in the maintained presence of D-serine) blocked the increase of current noise, reducing it to a level (0.80 pA^2) lower than the baseline level before D-serine (Figure 6d,e). CPP also blocked the inward current evoked by D-serine and resulted in a small outward current relative to the baseline recorded before D-serine (Figure 6d). That CPP reduced both the membrane noise and the inward current strongly suggests the presence of a baseline level of NMDAR-mediated activity in the absence of added D-serine. For a total of four A17s tested, there was a significant increase of current noise from 3.5 ± 1.4 pA^2 in control to 17.7 ± 6.2 pA^2 in the presence of D-serine (an average increase of ~530%; $p = 0.0151$, ratio paired t test, $n = 4$; Figure 6f). Three of the cells could be held long enough to add CPP to the bath solution. For these cells, CPP reduced the current noise to 1.01 ± 0.49 pA^2, a significant reduction from the D-serine condition ($p = 0.0400$), but not the baseline condition ($p = 0.8632$; adjusted p values, one-way ANOVA followed by Tukey's multiple comparison test; $n = 3$; Figure 6f). For all A17s tested in this way, D-serine also evoked an inward current with transient and sustained response components. The amplitude of the transient peak (relative to baseline) was 36 ± 13 pA (range 10–55 pA). For the three cells tested with CPP, the inward current evoked by D-serine was completely blocked and, for two of the cells, CPP evoked an apparent outward current relative to baseline. These results with CPP clearly suggested that both the

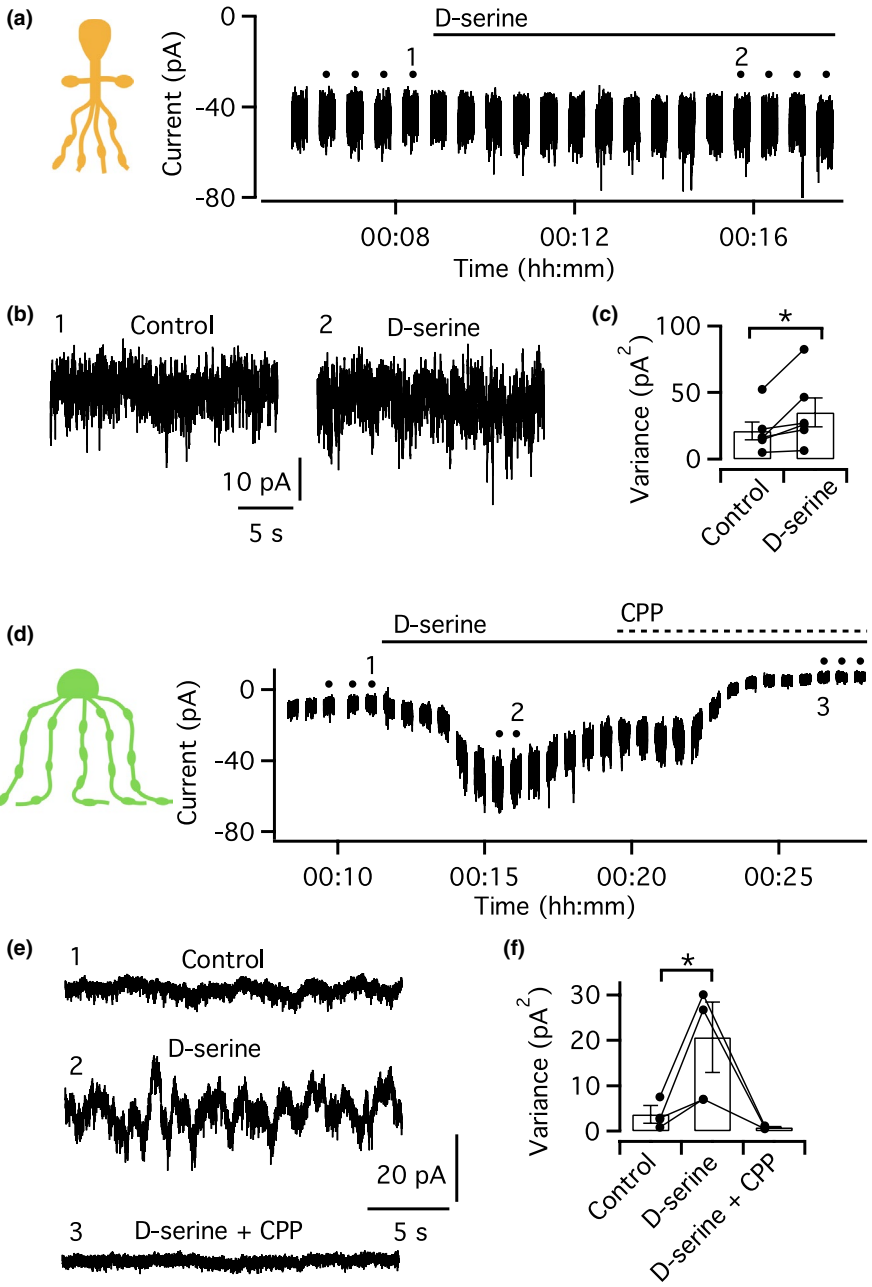

FIGURE 6 Co-agonist binding sites for NMDARs on AII and A17 amacrines in retinal slices are not saturated. (a) Series of 20-s epochs of current recorded from an AII amacrine. After establishing a baseline, the NMDAR co-agonist D-serine (100 μM) was added to the bath solution. Note moderate increase of current noise and small inward current (relative to the baseline) evoked by D-serine. (b) Individual epochs of current recorded from AII amacrine in (a); in control (1) and in the presence of D-serine (2). (c) Bar graph displays membrane current noise measured as variance in AII amacrines ($n = 6$ cells) in control and in D-serine. Note significant increase of noise evoked by D-serine. (d) Series of 20-s epochs of current recorded from an A17 amacrine. After establishing a baseline, D-serine (100 μM) was added to the bath solution. Note marked increase of noise and inward current evoked by D-serine. Subsequently, CPP (20 μM) was added to the bath solution to block NMDARs. Note apparent outward current (relative to baseline) and strong reduction of current noise evoked by CPP. (e) Individual epochs of current recorded from A17 amacrine in (d); in control (1), in the presence of D-serine (2), and in the presence of D-serine + CPP (3). (f) Bar graph displays membrane current noise measured as variance in A17 amacrines ($n = 4$) in control, in D-serine, and in D-serine + CPP (only three of the cells were recorded with CPP added). Note significant increase of noise evoked by D-serine (compared with control) and subsequent decrease of noise evoked by CPP (compared with D-serine)

increase of current noise and the inward current evoked by D-serine were due to increased activation of NMDARs in A17 amacrines.

The above experiments suggested that, for both AII and A17 amacrines, the endogenous co-agonist binding site for NMDARs was not saturated, opening up the possibility

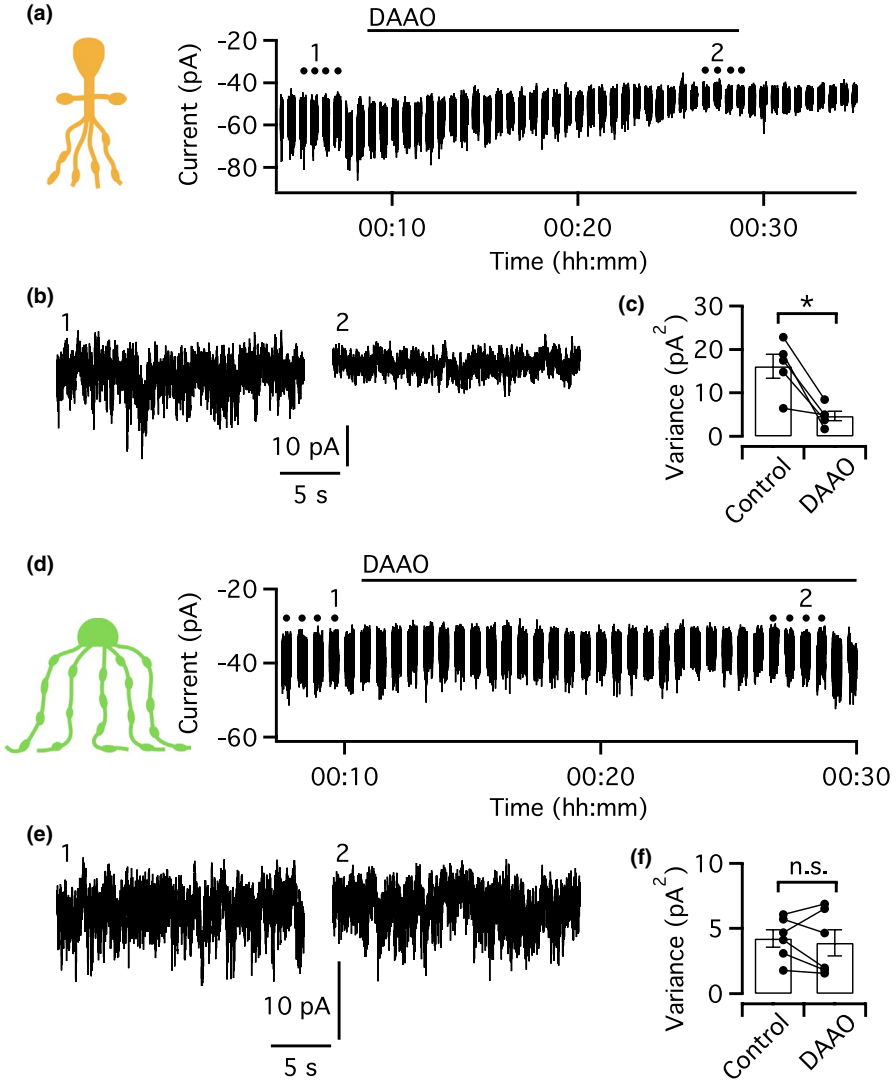

FIGURE 7 D-serine is the endogenous co-agonist for NMDARs on AII amacrines. (a) Series of 20-s epochs of current recorded from an AII amacrine. Here and in (d), D-serine was not included in the bath solution. After establishing a baseline, the enzyme D-amino acid oxidase (DAAO; 0.29 U/ml) was added to the bath solution to degrade any endogenous D-serine. Note reduction of current noise following application of DAAO. (b) Individual epochs of current recorded from AII amacrine in *A*; in control (1) and in the presence of DAAO (2). (c) Bar graph displays membrane current noise measured as variance in AII amacrines ($n = 5$ cells) in control and in DAAO. Note significant decrease of noise evoked by DAAO. (d) Series of 20-s epochs of current recorded from an A17 amacrine. After establishing a baseline, the enzyme D-amino acid oxidase (DAAO) was added to the bath solution. Note similarity of current noise before and after application of DAAO. (e) Individual epochs of current recorded from A17 amacrine in (d); in control (1) and in the presence of DAAO (2). (f) Bar graph displays membrane current noise measured as variance in A17 amacrines ($n = 6$ cells) in control and in DAAO. Note no significant difference of noise between the two conditions

that modulation of co-agonist levels has the potential to regulate the activation of these receptors (cf. Kalbaugh et al., 2009). The D-serine-evoked increase of current noise and inward current was considerably larger for A17s than for AIIs, possibly suggesting that the endogenous co-agonist for A17s is maintained at a lower level than that for AIIs. It is difficult, however, to make a direct comparison because the total number of receptors is likely to be higher for A17s, given the larger total length of processes for this wide-field amacrine compared with the narrow-field AII. Related to this, the smaller dendritic trees and shorter branches of the AII likely result in a lower extent of electrotonic filtering, with increases of NMDAR-mediated channel gating more easily detected as increased current noise, before becoming strong enough to be accompanied by a clear increase in inward current (relative to baseline). It is also important to note that in the retinal slice preparation, as used here, levels of endogenous co-agonists could be lower than under normal, physiological conditions (in situ) because of washout.

3.5 | D-serine is the likely co-agonist at extrasynaptic NMDARs of AII amacrine cells

It has been proposed that D-serine primarily acts at synaptic NMDARs and glycine primarily acts at extrasynaptic NMDARs (Papouin et al., 2012), but there is also evidence that either or both of these co-agonists can act on NMDARs throughout the CNS, with no preference for synaptic versus extrasynaptic receptors (Li et al., 2013; Mothet et al., 2015; Rosenberg et al., 2013). For the NMDARs on AII and A17 amacrines, which appear to be exclusively extrasynaptic, there is no information about which co-agonists are involved, or whether there may be a preferred co-agonist for either receptor population based on endogenous availability.

To investigate whether D-serine or glycine might be the physiologically relevant co-agonist for NMDARs on AII or A17 amacrines, we performed a series of recordings with the enzyme DAAO that degrades endogenous D-serine (Dixon & Kleppe, 1965; Molla et al., 2006). If treatment with DAAO decreases membrane current noise, it would suggest that D-serine is the predominant endogenous co-agonist at the corresponding NMDARs (Li et al., 2013; Mothet et al., 2015; Panatier et al., 2006; Papouin et al., 2012). For these experiments, D-serine was not included in the bath solution, which contained CNQX, bicuculline, strychnine, and TTX. For the AII illustrated in Figure 7a, adding DAAO to the bath solution (0.29 U/ml) resulted in a slowly developing decrease of current noise, from 14.8 pA^2 in control to 3.7 pA^2 after ~20 min in DAAO (a reduction of ~74%; each average calculated from four epochs, Figure 7a). The strong decrease of noise can be seen more clearly for the representative epochs illustrated at an expanded scale in Figure 7b (1: control, 2: DAAO). The noise decrease was accompanied by a slowly developing outward current (~12 pA peak amplitude) relative to the baseline. For five AIIs, there was a significant reduction of current noise from 16.1 ± 2.7 pA^2 in control to 4.7 ± 1.1 pA^2 after ~20 min in DAAO (an average reduction of 65%; $p = 0.0224$, ratio paired t test, $n = 5$; Figure 7c). For the same cells, the average outward current (relative to baseline) evoked by DAAO was 14.1 ± 5.0 pA (with all cells displaying an outward current relative to baseline). Thus, enzymatic degradation of D-serine was accompanied by marked reduction in current noise for AII amacrines, strongly suggesting that D-serine is the endogenous co-agonist at NMDARs on these cells.

In contrast, for A17 amacrines tested in the same way, DAAO had no clear effect on membrane current noise. For the A17 illustrated in Figure 7d, the noise in control was 5.7 pA^2, and after ~20 min in DAAO, it was 4.7 pA^2 (a reduction of ~19%; each average calculated from four epochs, Figure 7d). The relatively similar noise level in the two conditions can be observed for the representative epochs illustrated at an expanded scale in Figure 7e (1: control, 2: DAAO). For this cell, the difference in the current magnitude between control and DAAO was only 1.5 pA (Figure 7d). For six A17s, there was no significant difference between the current noise in control (4.24 ± 0.66 pA^2) and after ~20 min in DAAO (3.90 ± 0.99 pA^2; $p = 0.2888$, ratio paired t test, $n = 6$; Figure 7f). For the same A17 cells, adding DAAO was accompanied by minor changes in the current magnitude. Five cells displayed a small outward current (7.4 ± 2.9 pA), and one cell displayed a small inward current (3.8 pA) relative to baseline. The lack of effect of DAAO on the current noise for A17 amacrines suggested that D-serine is not likely to be the predominant endogenous co-agonist for NMDARs on these cells. Rather, it suggests that glycine is the major endogenous co-agonist.

4 | DISCUSSION

AII and A17 amacrine cells are the main inhibitory interneurons of the rod pathway microcircuit, and each cell type expresses NMDARs with an exclusively extrasynaptic location. NMDARs of AII amacrines contain GluN2B subunits, whereas those of A17 amacrines contain GluN2A subunits (Veruki et al., 2019). As the specific GluN2 subunit strongly influences the functional properties of NMDARs (Paoletti et al., 2013), this suggests that these receptors are exploited for different purposes in AII and A17 amacrines which receive simultaneous synaptic glutamatergic input from rod bipolar cells. Here, we reveal that the sources of glutamate and the endogenous co-agonists that activate these receptor populations are also different, adding to their divergent characteristics. Our results suggest that NMDARs on AIIs are activated by glutamate that arises from vesicular release from neurons, and that D-serine is the endogenous co-agonist. This contrasts with A17s, where the source of glutamate is predominantly non-vesicular, originating from glial cells, and the endogenous co-agonist is likely to be glycine. These results are summarized by the schematic in Figure 8. Below we discuss the basis for our interpretations and their functional implications.

4.1 | Different sources of glutamate for extrasynaptic NMDARs

In general, synaptic receptors are exclusively activated by neurotransmitter released from directly apposed, morphologically specialized presynaptic terminals. For extrasynaptic receptors, the source of neurotransmitter is more complicated and can encompass both neurotransmitter originating from synaptic spillover at varying distances from the receptors and neurotransmitter originating from non-neuronal sources. Extracellular glutamate originates from vesicular

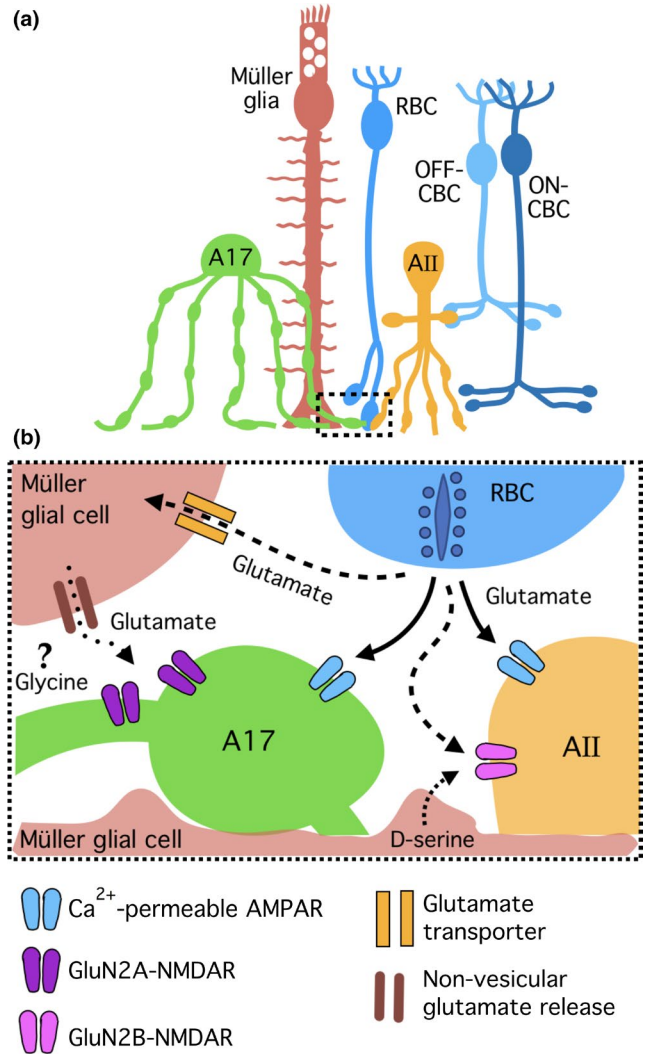

FIGURE 8 Different sources of glutamate and different endogenous co-agonists activate NMDARs on AII and A17 amacrines. (a) Schematic illustration of the major components of the classical rod pathway microcircuit in mammalian retina: A17 amacrine (green), AII amacrine (yellow), rod bipolar cell (RBC; medium blue), OFF-cone bipolar cell (OFF-CBC; light blue), and ON-cone bipolar cell (ON-CBC; dark blue). A Müller glial cell (light red) is also included. Photoreceptors are omitted for simplicity. (b) Magnified view of cellular interactions mediated by neurotransmitters, neurotransmitter receptors, and transporters in region of (a) demarcated by dashed rectangle. Synaptic release of glutamate from RBC (solid black arrows) activates postsynaptic Ca^{2+}-permeable AMPA receptors on A17 and AII amacrines. Glutamate diffusing into neuropil after synaptic release (dashed black arrows) activates extrasynaptic NMDARs on AII amacrines and is removed by uptake into Müller glial cells. Müller glial cells release glutamate (dotted black arrow) via unknown non-vesicular mechanism(s). Extrasynaptic NMDARs of A17s are activated by ambient glutamate from a glial source and glycine (from an unknown neuronal source) as the endogenous co-agonist. Extrasynaptic NMDARs of AIIs are activated by ambient glutamate originating from a neuronal source, with D-serine, released from Müller glial cells (small black arrow) or potentially astrocytes in the nerve fiber layer, as the endogenous co-agonist. Many details have been omitted for simplicity. For example, AII amacrines express extrasynaptic NMDARs not only on their distal arboreal dendrites, but also on proximal arboreal and lobular dendrities. In addition, neuronal sources of glutamate correspond not only to glutamate released from RBCs, but also from ON- and OFF- cone bipolar cells

release from neurons and from vesicular and non-vesicular release from glial cells (Hamilton & Attwell, 2010). The concentration of extracellular glutamate is estimated to be from 0.03 to 3 μM (Vizi et al., 2010), a level sufficient to activate NMDARs (Traynelis et al., 2010). For the extrasynaptic NMDARs on AII and A17 amacrines, potential sources of glutamate include spillover following synaptic release from rod and cone bipolar cells (Veruki et al., 2006; Wersinger et al., 2006) and release of glutamate from glial cells (Bringmann et al., 2006).

We manipulated extracellular glutamate by blocking vesicular uptake with bafilomycin or by blocking the enzymatic conversion of glutamate to glutamine within glial cells with MSO. Bafilomycin will reduce the concentration of ambient glutamate originating from vesicular release (from neurons and glia). MSO will reduce the concentration of ambient glutamate originating from neurons, but not from glia. For the NMDARs on AII amacrine cells, incubation in bafilomycin or MSO resulted in decreased NMDAR-mediated current noise, strongly suggesting that the source of glutamate is both vesicular and neuronal. For glutamate that originates from non-vesicular release from glia, neither pharmacological agent should lead to a significant decrease of the ambient concentration of glutamate and, thus, little change in NMDAR-mediated current noise would be expected. This is consistent with our observations for A17 amacrines, suggesting that NMDARs on these cells are activated by non-vesicular glutamate released from glial cells. A third outcome, when using bafilomycin and MSO, could reveal that the source of glutamate was due to vesicular release from glial cells. In this case, bafilomycin would reduce the available glutamate (and reduce NMDAR-mediated activity), but MSO would not. However, this was not observed in our study.

Glial sources of glutamate have been shown to activate extrasynaptic NMDARs in hippocampal CA1 pyramidal cells (Fellin et al., 2004; Gómez-Gonzalo et al., 2018; Le Meur et al., 2007). In contrast, spillover of glutamate released synaptically from neurons has been shown to activate extrasynaptic NMDARs on granule cells in the dentate gyrus (Dalby & Mody, 2003), retinal ganglion cells (Chen & Diamond, 2002), and CA1 pyramidal cells (Diamond, 2001). For AII and A17 amacrines, the functional significance of distinct sources of glutamate is not readily apparent, but suggests that the extrasynaptic NMDARs on these neurons are activated independently of each other.

4.2 | Endogenous co-agonists for extrasynaptic NMDARs

Both D-serine and glycine have been identified as co-agonists at NMDARs, but it is generally not known whether one or the other fulfills that role for a specific NMDAR population under physiological conditions (Mothet et al., 2015). The suggestion that D-serine primarily acts at synaptic GluN2A-containing receptors, whereas glycine primarily acts at extrasynaptic GluN2B-containing receptors (e.g., Le Bail et al., 2015; Papouin et al., 2012), seems to be violated by multiple exceptions, including the lack of correspondence between the molecular identity of the GluN2 subunit and the synaptic versus extrasynaptic location (e.g., Panatier et al., 2006). GluN2A-containing NMDARs have a slightly higher affinity for D-serine and an approximately tenfold lower affinity for glycine than GluN2B-containing NMDARs (Kutsuwada et al., 1992; Priestley et al., 1995). These differences in affinity are relatively small, however, and the status of D-serine or glycine as the endogenous co-agonist for a given receptor population may well depend on other factors such as temporal and spatial availability related to release and uptake (Mothet et al., 2015).

D-serine is synthesized by the enzyme serine racemase and can be released by both neurons (glutamatergic and GABAergic) and glia (Coyle et al., 2020). In the retina, however, D-serine and serine racemase have only been detected in Müller glial cells and in astrocytes in the nerve fiber layer, but not in neurons (Stevens et al., 2003; Williams et al., 2006). In our experiments, enzymatic degradation of D-serine markedly reduced NMDAR-mediated noise for AII amacrines, strongly suggesting that D-serine is the endogenous co-agonist for the NMDARs on these cells. In contrast, for A17 amacrines recorded in the same conditions, degrading D-serine had no effect on NMDAR-mediated noise, suggesting that glycine, rather than D-serine, is likely to be the predominant endogenous co-agonist.

Glycine would seem to be readily available in the retina, as ~50% of amacrine cells are glycinergic. Levels of extracellular glycine are tightly regulated in the retina by glycine transporters (GlyTs) that are exclusively located on glycinergic amacrine cells, including the AII (Menger et al., 1998; Pow & Hendrickson, 1999). There is no evidence that glia in the retina either take up or release glycine (Reye et al., 2001). Synaptically released glycine is thought to be the co-agonist at synaptic NMDARs on retinal ganglion cells (Kalbaugh et al., 2009), and the activation of GlyT1 has been shown to regulate NMDAR activity in ganglion cells (Reed et al., 2009). Although our interpretation that glycine is the co-agonist at NMDARs on A17s is reasonable, direct evidence for this remains to be obtained.

4.3 | Activation of extrasynaptic NMDARs on A17 amacrines

The source of non-vesicular glutamate that plays the predominant role in activating NMDARs on A17 amacrines remains unkown, but based on our results with MSO, it is reasonable to speculate that it corresponds to glial cells. A number of different mechanisms have been proposed for non-vesicular release of glutamate from astrocytes, including cystine-glutamate exchange (Baker et al., 2002) and efflux of cytosolic glutamate through either gap junction hemichannels (e.g., Ye et al., 2003), the conductance pore of $P2X_7$ receptors (e.g., Duan et al., 2003), or volume-sensitive organic anion channels (Kimelberg et al., 1990; Seki et al., 1999). In addition, under pathological conditions like ischemia, there is evidence for release via reversal of glutamate transporters (Rossi et al., 2000). In the mammalian retina, the relevant glial cells are Müller cells and conventional astrocytes (in the nerve fiber and ganglion cell layers; Stone & Dreher, 1987). Müller cells span the entire thickness of the retina and have the highest glutamate uptake capability in this tissue (Rauen et al., 1998). There is evidence that, at least under some conditions, Müller cells can release glutamate via both vesicular and non-vesicular mechanisms (Reichenbach & Bringmann, 2013), both of which can be Ca^{2+}-dependent (Slezak et al., 2012).

The processes of Müller cells are expected to be in close contact with the dendrites of both AII and A17 amacrines, but we are unaware of data that could suggest a differential localization of relevant molecular mechanisms within subcellular compartments of Müller cells that would indicate a differential relationship with either neuron. For astrocytes in the nerve fiber and ganglion cell layers, there also seems to be a paucity of relevant data, but the proximity of the processes of these cells to the dendritic processes of A17 amacrine cells in stratum 5 of the inner plexiform layer is intriguing.

4.4 | Functional roles for extrasynaptic NMDARs on AII and A17 amacrines

Previous work from our laboratory suggests that GluN2B-containing NMDARs on AII amacrines are co-localized with the gap junction protein connexin 36 (Veruki et al., 2019; see also Kothmann et al., 2012), supporting the hypothesis that the electrical synapses these cells make with each other and with ON-cone bipolar cells (Veruki & Hartveit, 2002a, 2002b) can be modulated by NMDAR activation (Kothmann et al., 2012). A neuronal source for the glutamate that activates these receptors suggests a mechanism that links gap junction modulation to changes in neuronal activity that impact levels of extracellular glutamate. Release of D-serine from retinal glial cells can also be modulated in an

activity-dependent manner, via activation of non-NMDARs (Sullivan & Miller, 2010) and by light stimulation (Gustafson et al., 2015; Sullivan et al., 2011).

A17 amacrine cells provide feedback inhibition to the axon terminals of rod bipolar cells through release of GABA (Chávez et al., 2006; Hartveit, 1999). We have previously demonstrated that activation of NMDARs can increase the excitability of A17 amacrines and enhance the inhibition of rod bipolar cells (Veruki et al., 2019). It is not clear, however, why a non-neuronal source of glutamate (coupled with a neuronal source of the co-agonist glycine) might be functionally relevant for the activation of these NMDARs which can modulate the feedback inhibition.

Although the absolute magnitude of membrane current noise appears larger in AIIs than in A17s, both in control and after blocking NMDARs with CPP, the relative noise reduction evoked by CPP (without treatment with bafilomycin or MSO) is quite similar for the two cell types (~80% block). The most likely explanation for the different noise levels (with or without blocked NMDARs) is the difference in intrinsic properties of these cell types, specifically their different morphological properties and electrotonic structure. For the wide-field A17 amacrines, with their long and thin processes, the extent of electrotonic (low-pass) filtering is expected to be much stronger than for the AII amacrine cells.

Even though GluN2A and GluN2B subunits have been localized to different regions of the dendritic trees of A17 and AII amacrine cells, respectively, our understanding of their exact subcellular distribution is incomplete. Further experimental work to investigate the subcellular distribution of the specific subunits, the cellular correlates (as well as the conditions and mechanisms of release) of the different sources of glutamate, and the functional consequences of activating extrasynaptic NMDARs on AII and A17 amacrines, is clearly required.

ACKNOWLEDGEMENTS

We thank Torhild Fjordheim Sunde and Áurea Castilho for excellent technical assistance. This study was supported by the Research Council of Norway (NFR 213776 and 261914 to M. L. Veruki).

CONFLICT OF INTEREST

No conflicts of interest, financial or otherwise, are declared by the authors.

AUTHOR CONTRIBUTIONS

PB performed experiments; EH contributed unpublished analytical tools; PB and MLV analyzed data and prepared figures; EH and MLV conceived and designed the research and wrote the manuscript; MLV supervised the project. All authors interpreted results and edited, revised, and approved the final version of the manuscript.

PEER REVIEW

The peer review history for this article is available at https://publons.com/publon/10.1111/ejn.15325.

DATA AVAILABILITY STATEMENT

The data that support the findings of this study are available from the corresponding author upon reasonable request.

ORCID

Pablo Beltrán-Matas https://orcid.org/0000-0003-3817-5095
Espen Hartveit https://orcid.org/0000-0003-1798-1901
Margaret L. Veruki https://orcid.org/0000-0002-0532-144X

REFERENCES

Baker, D. A., Xi, Z. X., Shen, H., Swanson, C. J., & Kalivas, P. W. (2002). The origin and neuronal function of in vivo nonsynaptic glutamate. *Journal of Neuroscience*, *22*, 9134–9141.

Barbour, B., & Häusser, M. (1997). Intersynaptic diffusion of neurotransmitter. *Trends in Neurosciences*, *20*, 377–384.

Barnett, N. L., Pow, D. V., & Robinson, S. R. (2000). Inhibition of Müller cell glutamine synthetase rapidly impairs the retinal response to light. *Glia*, *30*, 64–73.

Bringmann, A., Pannicke, T., Grosche, J., Francke, M., Wiedemann, P., Skatchkov, S. N., Osborne, N. N., & Reichenbach, A. (2006). Müller cells in the healthy and diseased retina. *Progress in Retinal and Eye Research*, *25*, 397–424. https://doi.org/10.1016/j.preteyeres.2006.05.003

Castilho, Á., Ambrósio, A. F., Hartveit, E., & Veruki, M. L. (2015). Disruption of a neural microcircuit in the rod pathway of the mammalian retina by diabetes mellitus. *Journal of Neuroscience*, *35*, 5422–5433. https://doi.org/10.1523/JNEUROSCI.5285-14.2015

Cavelier, P., & Attwell, D. (2007). Neurotransmitter depletion by bafilomycin is promoted by vesicle turnover. *Neuroscience Letters*, *412*, 95–100. https://doi.org/10.1016/j.neulet.2006.10.040

Chávez, A. E., Singer, J. H., & Diamond, J. S. (2006). Fast neurotransmitter release triggered by Ca influx through AMPA-type glutamate receptors. *Nature*, *443*, 705–708. https://doi.org/10.1038/nature05123

Chen, S., & Diamond, J. S. (2002). Synaptically released glutamate activates extrasynaptic NMDA receptors on cells in the ganglion cell layer of rat retina. *Journal of Neuroscience*, *22*, 2165–2173. https://doi.org/10.1523/JNEUROSCI.22-06-02165.2002

Cowan, W. M., & Kandel, E. R. (2001). A brief history of synapses and synaptic transmission. In W. M. Cowan, T. C. Südhof, & C. F. Stevens (Eds.), *Synapses* (pp. 1–87). Johns Hopkins University Press.

Coyle, J. T., Balu, D., & Wolosker, H. (2020). D-serine, the shape-shifting NMDA receptor co-agonist. *Neurochemical Research*, *45*, 1344–1353. https://doi.org/10.1007/s11064-020-03014-1

Dalby, N. O., & Mody, I. (2003). Activation of NMDA receptors in rat dentate gyrus granule cells by spontaneous and evoked transmitter release. *Journal of Neurophysiology*, *90*, 786–797. https://doi.org/10.1152/jn.00118.2003

Diamond, J. S. (2001). Neuronal glutamate transporters limit activation of NMDA receptors by neurotransmitter spillover on CA1

pyramidal cells. *Journal of Neuroscience*, *21*, 8328–8338. https://doi.org/10.1523/JNEUROSCI.21-21-08328.2001

Dixon, M., & Kleppe, K. (1965). D-amino acid oxidase I. Dissociation and recombination of the holoenzyme. *Biochimica et Biophysica Acta*, *96*, 357–367. https://doi.org/10.1016/0005-2787(65)90556-3

Dröse, S., & Altendorf, K. (1997). Bafilomycins and concanamycins as inhibitors of V-ATPases and P-ATPases. *Journal of Experimental Biology*, *200*, 1–8. https://doi.org/10.1242/jeb.200.1.1

Duan, S., Anderson, C. M., Keung, E. C., Chen, Y., Chen, Y., & Swanson, R. A. (2003). P2X7 receptor-mediated release of excitatory amino acids from astrocytes. *Journal of Neuroscience*, *23*, 1320–1328.

Fellin, T., Pascual, O., Gobbo, S., Pozzan, T., Haydon, P. G., & Carmignoto, G. (2004). Neuronal synchrony mediated by astrocytic glutamate through activation of extrasynaptic NMDA receptors. *Neuron*, *43*, 729–743. https://doi.org/10.1016/j.neuron.2004.08.011

Fuxe, K., Dahlström, A., Höistad, M., Marcellino, D., Jansson, A., Rivera, A., Diaz-Cabiale, Z., Jacobsen, K., Tinner-Staines, B., Hagman, B., Leo, G., Staines, W., Guidolin, D., Kehr, J., Genedani, S., Belluardo, N., & Agnati, L. F. (2007). From the Golgi-Cajal mapping to the transmitter-based characterization of the neuronal networks leading to two modes of brain communication: Wiring and volume transmission. *Brain Research Reviews*, *55*, 17–54. https://doi.org/10.1016/j.brainresrev.2007.02.009

Gómez-Gonzalo, M., Zehnder, T., Requie, L. M., Bezzi, P., & Carmignoto, G. (2018). Insights into the release mechanism of astrocytic glutamate evoking in neurons NMDA receptor-mediated slow depolarizing inward currents. *Glia*, *66*, 2188–2199. https://doi.org/10.1002/glia.23473

Gustafson, E. G., Stevens, E. S., & Miller, R. F. (2015). Dynamic regulation of D-serine release in the vertebrate retina. *Journal of Physiology*, *593*, 843–856.

Hamilton, N., & Attwell, D. (2010). Do astrocytes really exocytose neurotransmitters? *Nature Reviews Neuroscience*, *11*, 227–238. https://doi.org/10.1038/nrn2803

Hansen, K. B., Yi, F., Perszyk, R. E., Furukawa, H., Wollmuth, L. P., Gibb, A. J., & Traynelis, S. F. (2018). Structure, function, and allosteric modulation of NMDA receptors. *Journal of General Physiology*, *150*, 1081–1105. https://doi.org/10.1085/jgp.201812032

Harrison, J., & Jahr, C. E. (2003). Receptor occupancy limits synaptic depression at climbing fiber synapses. *Journal of Neuroscience*, *23*, 377–383. https://doi.org/10.1523/JNEUROSCI.23-02-00377.2003

Hartveit, E. (1999). Reciprocal synaptic interactions between rod bipolar cells and amacrine cells in the rat retina. *Journal of Neurophysiology*, *81*, 2923–2936. https://doi.org/10.1152/jn.1999.81.6.2923

Hartveit, E., & Veruki, M. L. (1997). AII amacrine cells express functional NMDA receptors. *NeuroReport*, *8*, 1219–1223. https://doi.org/10.1097/00001756-199703240-00032

Johnson, J. W., & Ascher, P. (1987). Glycine potentiates the NMDA response in cultured mouse brain neurons. *Nature*, *325*, 529–531. https://doi.org/10.1038/325529a0

Kalbaugh, T. L., Zhang, J., & Diamond, J. S. (2009). Coagonist release modulates NMDA receptor subtype contributions at synaptic inputs to retinal ganglion cells. *Journal of Neuroscience*, *29*, 1469–1479. https://doi.org/10.1523/JNEUROSCI.4240-08.2009

Kimelberg, H. K., Goderie, S. K., Higman, S., Pang, S., & Waniewski, R. A. (1990). Swelling-induced release of glutamate, aspartate, and taurine from astrocyte cultures. *Journal of Neuroscience*, *10*, 1583–1591. https://doi.org/10.1523/JNEUROSCI.10-05-01583.1990

Kleckner, N. W., & Dingledine, R. (1988). Requirement for glycine in activation of NMDA-receptors expressed in Xenopus oocytes. *Science*, *241*, 835–837. https://doi.org/10.1126/science.2841759

Kolb, H., & Famiglietti, E. V. (1974). Rod and cone pathways in the inner plexiform layer of cat retina. *Science*, *186*, 47–49. https://doi.org/10.1126/science.186.4158.47

Kothmann, W. W., Trexler, E. B., Whitaker, C. M., Li, W., Massey, S. C., & O'Brien, J. (2012). Nonsynaptic NMDA receptors mediate activity-dependent plasticity of gap junctional coupling in the AII amacrine cell network. *Journal of Neuroscience*, *32*, 6747–6759. https://doi.org/10.1523/JNEUROSCI.5087-11.2012

Kutsuwada, T., Kashiwabuchi, N., Mori, H., Sakimura, K., Kushiya, E., Araki, K., Meguro, H., Masaki, H., Kumanishi, T., Arakawa, M., & Mishina, M. (1992). Molecular diversity of the NMDA receptor channel. *Nature*, *358*, 36–41. https://doi.org/10.1038/358036a0

Laake, J. H., Slyngstad, T. A., Haug, F.-M.-S., & Ottersen, O. P. (1995). Glutamine from glial cells is essential for the maintenance of the nerve terminal pool of glutamate: Immunogold evidence from hippocampal slice cultures. *Journal of Neurochemistry*, *65*, 871–881. https://doi.org/10.1046/j.1471-4159.1995.65020871.x

Le Bail, M., Martineau, M., Sacchi, S., Yatsenko, N., Radzishevsky, I., Conrod, S., Ait Ouares, K., Wolosker, H., Pollegioni, L., Billard, J. M., & Mothet, J. P. (2015). Identity of the NMDA receptor coagonist is synapse specific and developmentally regulated in the hippocampus. *Proceedings of the National Academy of Sciences of the United States of America*, *112*, E204–E213. https://doi.org/10.1073/pnas.1416668112

Le Meur, K., Galante, M., Angulo, M. C., & Audinat, E. (2007). Tonic activation of NMDA receptors by ambient glutamate of non-synaptic origin in the rat hippocampus. *Journal of Physiology*, *580*, 373–383. https://doi.org/10.1113/jphysiol.2006.123570

Lewis, G. P., Erickson, P. A., Kaska, D. D., & Fisher, S. K. (1988). An immunocytochemical comparison of Müller cells and astrocytes in the cat retina. *Experimental Eye Research*, *47*, 839–853. https://doi.org/10.1016/0014-4835(88)90067-X

Li, Y., Sacchi, S., Pollegioni, L., Basu, A. C., Coyle, J. T., & Bolshakov, V. Y. (2013). Identity of endogenous NMDAR glycine site agonist in amygdala is determined by synaptic activity level. *Nature Communications*, *4*, 1760. https://doi.org/10.1038/ncomms2779

Menger, N., Pow, D. V., & Wässle, H. (1998). Glycinergic amacrine cells of the rat retina. *The Journal of Comparative Neurology*, *401*, 34–46. https://doi.org/10.1002/(SICI)1096-9861(19981109)401:1<34:AID-CNE3>3.0.CO;2-P

Molla, G., Sacchi, S., Bernasconi, M., Pilone, M. S., Fukui, K., & Pollegioni, L. (2006). Characterization of human D-amino acid oxidase. *FEBS Letters*, *580*, 2358–2364.

Monyer, H., Burnashev, N., Laurie, D. J., Sakmann, B., & Seeburg, P. H. (1994). Developmental and regional expression in the rat brain and functional properties of four NMDA receptors. *Neuron*, *12*, 529–540. https://doi.org/10.1016/0896-6273(94)90210-0

Mørkve, S. H., Veruki, M. L., & Hartveit, E. (2002). Functional characteristics of non-NMDA-type ionotropic glutamate receptor channels in AII amacrine cells in rat retina. *Journal of Physiology*, *542*, 147–165. https://doi.org/10.1113/jphysiol.2002.020305

Mothet, J. P., Bail, M. L., & Billard, J. M. (2015). Time and space profiling of NMDA receptor co-agonist functions. *Journal of Neurochemistry*, *135*, 210–225. https://doi.org/10.1111/jnc.13204

Mothet, J. P., Parent, A. T., Wolosker, H., Brady, R. O., Linden, D. J., Ferris, C. D., Rogawski, M. A., & Snyder, S. H. (2000). D-Serine is an endogenous ligand for the glycine site of the N-methyl-D-aspartate

receptor. *Proceedings of the National Academy of Sciences of the United States of America*, *97*, 4926–4931. https://doi.org/10.1073/pnas.97.9.4926

Muller, E., Le-Corronc, H., & Legendre, P. (2008). Extrasynaptic and postsynaptic receptors in glycinergic and GABAergic neurotransmission: A division of labor? *Front Mol Neurosci*, *1*, 3. https://doi.org/10.3389/neuro.02.003.2008

Nelson, R., & Kolb, H. (1985). A17, A broad-field amacrine cell in the rod system of the cat retina. *Journal of Neurophysiology*, *54*, 592–614. https://doi.org/10.1152/jn.1985.54.3.592

Nowak, L., Bregestovski, P., Ascher, P., Herbet, A., & Prochiantz, A. (1984). Magnesium gates glutamate-activated channels in mouse central neurones. *Nature*, *307*, 462–465. https://doi.org/10.1038/307462a0

Panatier, A., Theodosis, T., Mothet, J. P., Touquet, B., Pollegioni, L., Poulain, D. A., & Oliet, S. H. R. (2006). Glia-derived D-serine controls NMDA receptor activity and synaptic memory. *Cell*, *125*, 775–784. https://doi.org/10.1016/j.cell.2006.02.051

Paoletti, P., Bellone, C., & Zhou, Q. (2013). NMDA receptor subunit diversity: Impact on receptor properties, synaptic plasticity and disease. *Nature Reviews Neuroscience*, *14*, 383–400. https://doi.org/10.1038/nrn3504

Papouin, T., Ladépêche, L., Ruel, J., Sacchi, S., Labasque, M., Hanini, M., Groc, L., Pollegioni, L., Mothet, J. P., & Oliet, S. H. (2012). Synaptic and extrasynaptic NMDA receptors are gated by different endogenous coagonists. *Cell*, *150*, 633–646. https://doi.org/10.1016/j.cell.2012.06.029

Papouin, T., & Oliet, S. H. R. (2014). Organization, control and function of extrasynaptic NMDA receptors. *Philosophical Transactions of the Royal Society B: Biological Sciences*, *369*, 20130601. https://doi.org/10.1098/rstb.2013.0601

Pow, D. V., & Hendrickson, A. E. (1999). Distribution of the glycine transporter glyt-1 in mammalian and nonmammalian retinae. *Visual Neuroscience*, *16*, 231–239.

Pow, D. V., & Robinson, S. R. (1994). Glutamate in some retinal neurons is derived solely from glia. *Neuroscience*, *60*, 355–366. https://doi.org/10.1016/0306-4522(94)90249-6

Priestley, T., Laughton, P., Myers, J., Le Bourdellés, B., Kerby, J., & Whiting, P. J. (1995). Pharmacological properties of recombinant human *N*-methyl-D-aspartate receptors comprising NR1a/NR2A and NR1a/NR2B subunit assemblies expressed in permanently transfected mouse fibroblast cells. *Molecular Pharmacology*, *48*, 841–848.

Rauen, T., Taylor, W. R., Kuhlbrodt, K., & Wiessner, M. (1998). High-affinity glutamate transporters in the rat retina: A major role of the glial glutamate transporter GLAST-1 in transmitter clearance. *Cell and Tissue Research*, *291*, 19–31. https://doi.org/10.1007/s004410050976

Reed, B. T., Sullivan, S. J., Tsai, G., Coyle, J. T., Esguerra, M., & Miller, R. F. (2009). The glycine transporter GlyT1 controls *N*-methyl-D-aspartic acid receptor coagonist occupancy in the mouse retina. *European Journal of Neuroscience*, *30*, 2308–2317. https://doi.org/10.1111/j.1460-9568.2009.07020.x

Reichenbach, A., & Bringmann, A. (2013). New functions of Müller cells. *Glia*, *61*, 651–678. https://doi.org/10.1002/glia.22477

Reye, P., Penfold, P., & Pow, D. V. (2001). Glyt-1 expression in cultured human Müller cells and intact retinae. *Glia*, *34*, 311–315. https://doi.org/10.1002/glia.1064

Riepe, R. E., & Norenburg, M. D. (1977). Müller cell localisation of glutamine synthetase in rat retina. *Nature*, *268*, 654–655. https://doi.org/10.1038/268654a0

Rosenberg, D., Artoul, S., Segal, A. C., Kolodney, G., Radzishevsky, I., Dikopoltsev, E., Foltyn, V. N., Inoue, R., Mori, H., Billard, J.-M., & Wolosker, H. (2013). Neuronal D-serine and glycine release via the Asc-1 transporter regulates NMDA receptor-dependent synaptic activity. *Journal of Neuroscience*, *33*, 3533–3544. https://doi.org/10.1523/JNEUROSCI.3836-12.2013

Rossi, D. J., Oshima, T., & Attwell, D. (2000). Glutamate release in severe brain ischaemia is mainly by reversed uptake. *Nature*, *403*, 316–321. https://doi.org/10.1038/35002090

Rusakov, D. A., & Dityatev, A. E. (2014). Brain circuitry outside the synaptic cleft. *Philosophical Transactions of the Royal Society B: Biological Sciences*, *369*, 20130591. https://doi.org/10.1098/rstb.2013.0591

Sah, P., Hestrin, S., & Nicoll, R. A. (1989). Tonic activation of NMDA receptors by ambient glutamate enhances excitability of neurons. *Science*, *246*, 815–818. https://doi.org/10.1126/science.2573153

Schousboe, A. (2019). Metabolic signaling in the brain and the role of astrocytes in control of glutamate and GABA neurotransmission. *Neuroscience Letters*, *689*, 11–13. https://doi.org/10.1016/j.neulet.2018.01.038

Scimemi, A., Fine, A., Kullmann, D. M., & Rusakov, D. A. (2004). NR2B-containing receptors mediate cross talk among hippocampal synapses. *Journal of Neuroscience*, *24*, 4767–4777. https://doi.org/10.1523/JNEUROSCI.0364-04.2004

Seki, Y., Feustel, P. J., Keller, R. W. Jr, Tranmer, B. I., & Kimelberg, H. K. (1999). Inhibition of ischemia-induced glutamate release in rat striatum by dihydrokainate and an anion channel blocker. *Stroke*, *30*, 433–440.

Shimamoto, K., LeBrun, B., Yasuda-Kamatani, Y., Sakaitani, M., Shigeri, Y., Yumoto, N., & Nakajima, T. (1998). DL-*threo*-β-benzyloxyaspartate, a potent blocker of excitatory amino acid transporters. *Molecular Pharmacology*, *53*, 195–201.

Slezak, M., Grosche, A., Niemiec, A., Tanimoto, N., Pannicke, T., Münch, T. A., Crocker, B., Isope, P., Härtig, W., Beck, S. C., Huber, G., Ferracci, G., Perraut, M., Reber, M., Miehe, M., Demais, V., Lévêque, C., Metzger, D., Szklarczyk, K., … Pfrieger, F. W. (2012). Relevance of exocytotic glutamate release from retinal glia. *Neuron*, *74*, 504–516. https://doi.org/10.1016/j.neuron.2012.03.027

Stevens, E. R., Esguerra, M., Kim, P. M., Newman, E. A., Snyder, S. H., Zahs, K. R., & Miller, R. F. (2003). D-serine and serine racemase are present in the vertebrate retina and contribute to the physiological activation of NMDA receptors. *Proceedings of the National Academy of Sciences of the United States of America*, *100*, 6789–6794. https://doi.org/10.1073/pnas.1237052100

Stone, J., & Dreher, Z. (1987). Relationship between astrocytes, ganglion cells and vasculature of the retina. *The Journal of Comparative Neurology*, *255*, 35–49. https://doi.org/10.1002/cne.902550104

Strettoi, E., Dacheux, R. F., & Raviola, E. (1990). Synaptic connections of rod bipolar cells in the inner plexiform layer of the rabbit retina. *The Journal of Comparative Neurology*, *295*, 449–466. https://doi.org/10.1002/cne.902950309

Strettoi, E., Raviola, E., & Dacheux, R. F. (1992). Synaptic connections of the narrow-field, bistratified amacrine cell (AII) in the rabbit retina. *The Journal of Comparative Neurology*, *325*, 152–168.

Sullivan, S. J., Esguerra, M., Wickham, R. J., Romero, G. E., Coyle, J. T., & Miller, R. F. (2011). Serine racemase deletion abolishes light-evoked NMDA receptor currents in retinal ganglion cells. *Journal of Physiology*, *589*, 5997–6006. https://doi.org/10.1113/jphysiol.2011.217059

Sullivan, S. J., & Miller, R. F. (2010). AMPA receptor mediated D-serine release from retinal glial cells. *Journal of Neurochemistry*, *115*, 1681–1689. https://doi.org/10.1111/j.1471-4159.2010.07077.x

Sullivan, S. J., & Miller, R. F. (2012). AMPA receptor-dependent, light-evoked D-serine release acts on retinal ganglion cell NMDA receptors. *Journal of Neurophysiology*, *108*, 1044–1051.

Traynelis, S. F., Wollmuth, L. P., McBain, C. J., Menniti, F. S., Vance, K. M., Ogden, K. K., Hansen, K. B., Yuan, H., Myers, S. J., & Dingledine, R. (2010). Glutamate receptor ion channels: Structure, regulation, and function. *Pharmacological Reviews*, *62*, 405–496. https://doi.org/10.1124/pr.109.002451

Veruki, M. L., & Hartveit, E. (2002a). AII (rod) amacrine cells form a network of electrically coupled interneurons in the mammalian retina. *Neuron*, *33*, 935–946. https://doi.org/10.1016/S0896-6273(02)00609-8

Veruki, M. L., & Hartveit, E. (2002b). Electrical synapses mediate signal transmission in the rod pathway of the mammalian retina. *Journal of Neuroscience*, *22*, 10558–10566. https://doi.org/10.1523/JNEUROSCI.22-24-10558.2002

Veruki, M. L., Mørkve, S. H., & Hartveit, E. (2003). Functional properties of spontaneous EPSCs and non-NMDA receptors in rod amacrine (AII) cells in the rat retina. *Journal of Physiology*, *549*, 759–774. https://doi.org/10.1113/jphysiol.2003.039982

Veruki, M. L., Mørkve, S. H., & Hartveit, E. (2006). Activation of a presynaptic glutamate transporter regulates synaptic transmission through electrical signaling. *Nature Neuroscience*, *9*, 1388–1396. https://doi.org/10.1038/nn1793

Veruki, M. L., Zhou, Y., Castilho, Á., Morgans, C. W., & Hartveit, E. (2019). Extrasynaptic NMDA receptors on rod pathway amacrine cells: Molecular composition, activation, and signaling. *Journal of Neuroscience*, *39*, 627–650. https://doi.org/10.1523/JNEUROSCI.2267-18.2018

Vizi, E. S., Fekete, A., Karoly, R., & Mike, A. (2010). Non-synaptic receptors and transporters involved in brain functions and targets of drug treatment. *British Journal of Pharmacology*, *160*, 785–809. https://doi.org/10.1111/j.1476-5381.2009.00624.x

Wersinger, E., Schwab, Y., Sahel, J.-A., Rendon, A., Pow, D. V., Picaud, S., & Roux, M. J. (2006). The glutamate transporter EAAT5 works as a presynaptic receptor in mouse rod bipolar cells. *The Journal of Physiology*, *577*, 221–234. https://doi.org/10.1113/jphysiol.2006.118281

Williams, S. M., Diaz, C. M., Macnab, L. T., Sullivan, R. K., & Pow, D. V. (2006). Immunocytochemical analysis of D-serine distribution in the mammalian brain reveals novel anatomical compartmentalizations in glia and neurons. *Glia*, *53*, 401–411. https://doi.org/10.1002/glia.20300

Winkler, B. S., Kapousta-Bruneau, N., Arnold, M. J., & Green, D. G. (1999). Effects of inhibiting glutamine synthetase and blocking glutamate uptake on b-wave generation in the isolated rat retina. *Visual Neuroscience*, *16*, 345–353.

Wolosker, H., Blackshaw, S., & Snyder, S. H. (1999). Serine racemase: A glial enzyme synthesizing D-serine to regulate glutamate-*N*-methyl-D-aspartate neurotransmission. *Proceedings of the National Academy of Sciences of the United States of America*, *96*, 13409–13414. https://doi.org/10.1073/pnas.96.23.13409

Wu, Y. W., Grebenyuk, S., McHugh, T. J., Rusakov, D. A., & Semyanov, A. (2012). Backpropagating action potentials enable detection of extrasynaptic glutamate by NMDA receptors. *Cell Reports*, *1*, 495–505. https://doi.org/10.1016/j.celrep.2012.03.007

Ye, Z. C., Wyeth, M. S., Baltan-Tekkok, S., & Ransom, B. R. (2003). Functional hemichannels in astrocytes: A novel mechanism of glutamate release. *Journal of Neuroscience*, *23*, 3588–3596. https://doi.org/10.1523/JNEUROSCI.23-09-03588.2003

Zandt, B.-J., Liu, J. H., Veruki, M. L., & Hartveit, E. (2017). AII amacrine cells: Quantitative reconstruction and morphometric analysis of electrophysiologically identified cells in live rat retinal slices imaged with multi-photon excitation microscopy. *Brain Structure and Function*, *222*, 151–182. https://doi.org/10.1007/s00429-016-1206-0

Zhou, Q., Petersen, C. C., & Nicoll, R. A. (2000). Effects of reduced vesicular filling on synaptic transmission in rat hippocampal neurones. *The Journal of Physiology*, *525*, 195–206. https://doi.org/10.1111/j.1469-7793.2000.t01-1-00195.x

Zhou, Y., Tencerova, B., Hartveit, E., & Veruki, M. L. (2016). Functional NMDA receptors are expressed by both AII and A17 amacrine cells in the rod pathway of the mammalian retina. *Journal of Neurophysiology*, *115*, 389–403. https://doi.org/10.1152/jn.00947.2015

How to cite this article: Beltrán-Matas, P., Hartveit, E., & Veruki, M. L. (2021). Different glutamate sources and endogenous co-agonists activate extrasynaptic NMDA receptors on amacrine cells of the rod pathway microcircuit. *European Journal of Neuroscience*, 00, 1–19. https://doi.org/10.1111/ejn.15325